



Cite this: *RSC Adv.*, 2020, **10**, 15430

Received 24th January 2020  
 Accepted 11th March 2020

DOI: 10.1039/d0ra00762e  
[rsc.li/rsc-advances](http://rsc.li/rsc-advances)

## 1. Introduction

Nowadays, nanotechnology has been integrated into different areas of science as it provides various significant ways to meet scientific and medical problems. Nanotechnology, which is a branch of technology, works in the dimensions of less than 100 nm. It includes objects such as viruses of about 100 nm size down to glucose molecules of about 1 nm size. Therefore, it includes the study of structures at the molecular and atomic scales.<sup>1-4</sup> Assorted nano-materials may be categorized on the basis of their morphology and the presence of nano-pores, which is exemplified by dendrimers, nano-tubes, quantum dots, liposomes, nano-rods, nano-wires, fullerenes, nano-

spheres, nano-belts, nano-rings, nano-shells, and nano-capsules (Fig. 1).

Most of the works that have been reported during the last 20–30 years have focused on nanoparticles; thus, it is clear that there is a great interest in nanotechnology and the features of the materials at these scales. For example, nanotechnology can measure the surface area of 1 g of a powder at different spherical sizes, and these data show that the surface area per gram rises exponentially below ~100 nm. This leads to a change in the phase of these materials such as the increase in the surface energy per gram of the material. This massive increase in the surface area can be applied for different purposes.<sup>5-10</sup>

Teeth within the oral cavity have various parts such as dentin, enamel, cementum, pulp, and periodontal ligament. Teeth cut and crush food to make it easy to swallow and digest. Furthermore, teeth empower self-confidence and improve the quality of life. Therefore, the loss of teeth due to a disease or decay can affect the eating pattern, speaking, or laughing. Thus, dentistry provides a lot of methods for protecting teeth.<sup>11-14</sup> These efforts suffer from key disadvantages, which require more efficient strategies and novel technologies in contemporary dentistry.<sup>15-18</sup>

Nanoparticles, unlike other biomaterials, present distinct biological properties and can be used in novel applications in restorative dentistry, prosthetic dentistry, endodontics, implantology, oral cancers, and periodontology. Nanoparticles have immense potential because of their antimicrobial, anti-viral, and antifungal properties. The incorporation of nanoparticles prevents biofilm build up over the composite, which avoids micro-leakage and secondary caries.<sup>19-21</sup> These nanoparticles enhance the mechanical properties of a restorative material and improve the overall bonding between dentin and biomaterials, thus affecting the bond strength. Nanoparticle-

<sup>a</sup>Institute of Research and Development, Duy Tan University, Da Nang, 550000, Viet Nam

<sup>b</sup>Department of Chemistry, Kerman Branch, Islamic Azad University, Kerman, Iran

<sup>c</sup>Nanobioelectrochemistry Research Center, Bam University of Medical Sciences, Bam, Iran. E-mail: [foroughi@iauk.ac.ir](mailto:foroughi@iauk.ac.ir); [armitaforutan@gmail.com](mailto:armitaforutan@gmail.com); Fax: +98 3433210051; Tel: +98 34331321750

<sup>d</sup>Student Research Committee, School of Public Health, Bam University of Medical Sciences, Bam, Iran

<sup>e</sup>Tehran Dental Branch, Islamic Azad University, Tehran, Iran

<sup>f</sup>Craniomaxillofacial Research Center, Tehran Medical Sciences, Islamic Azad University, Tehran, Iran

<sup>g</sup>Neuroscience Research Center, Institute of Neuropharmacology, Kerman University of Medical Sciences, Kerman, Iran

<sup>h</sup>Department of Pediatric Dentistry, School of Dentistry, Kerman University of Medical Sciences, Kerman, Iran

<sup>i</sup>Regional Centre of Advanced Technologies and Materials, Department of Physical Chemistry, Faculty of Science, Palacky University, Šlechtitelů 27, 783 71 Olomouc, Czech Republic

<sup>j</sup>Cell Therapy and Regenerative Medicine Comprehensive Center, Kerman University of Medical Sciences, Kerman, Iran



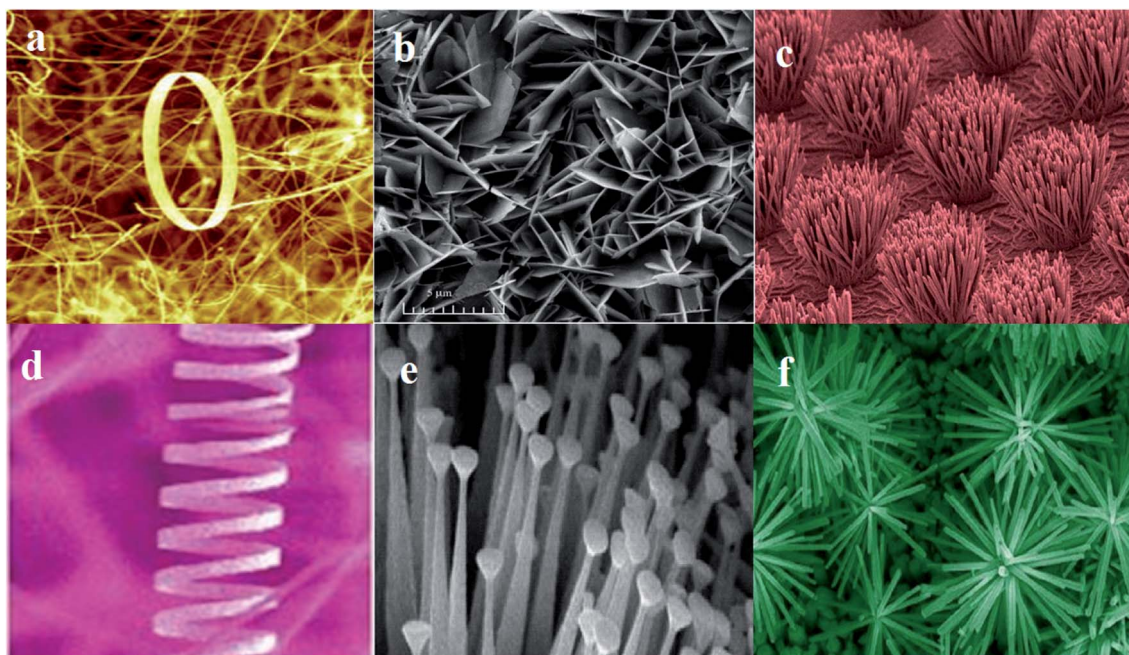


Fig. 1 Representative structures of some nano-materials: (a) nanorings,<sup>228</sup> (b) nanopellets,<sup>229</sup> (c) nanorods,<sup>230</sup> (d) nanosprings,<sup>228</sup> (e) nanonails,<sup>231</sup> (f) nanoflower.<sup>232</sup>

incorporated adhesive systems can be applied in orthodontic treatments to prevent white spot lesions. *In vitro* research has shown that these nanoparticles prevent crack propagation and improve the fracture toughness with dental ceramics, which negates the cracking of the porcelain restorations such as crowns, bridges, and veneers.<sup>22–25</sup> Although it is clear that nanoparticles can be effective due to their incorporation with dental biomaterials, to use them for clinical applications, *in vivo* results with long-term data are necessary. Besides the benefits of nanoparticles, the research on long-term *in vivo* results, methods of nanoparticle incorporation and characterization, and data on their long-term antibacterial action is needed for clinical applications.<sup>26–29</sup>

This paper provides an overview of the various kinds of nano-materials, their synthetic techniques, and characteristics including the science, implications, and up-to-date uses of nano-technology in dentistry. Novel designed materials introduced in the market as well as the summary of the contribution of dentists to the understanding of clinical relevance and efficiency of nano-materials is compared with those currently deployed in clinical practices.

## 2. Classification of nano-materials

The general classification of nano-materials comprising organic, inorganic, and carbon-based materials is presented below (Scheme 1).

### 2.1. Organic nano-materials

Organic nano-materials or polymers usually encompass dendrimers, micelles, liposomes, ferritin, *etc.*, which are biodegradable and non-toxic. A number of such particles, including

micelles and liposomes, have a hollow core, termed as nano-capsules that have the sensitivity towards thermal and electromagnetic radiations, including heat and light.<sup>30</sup> Such specific features render them a perfect option for drug delivery. Due to its stability, capacity, and delivery systems, the absorbed drug system determines the respective type of uses and efficacy, regardless of the physical properties, including dimensions, compositions, and surface morphologies. Organic nano-materials have widespread usage in biomedicine for targeted drug delivery.<sup>31–35</sup>

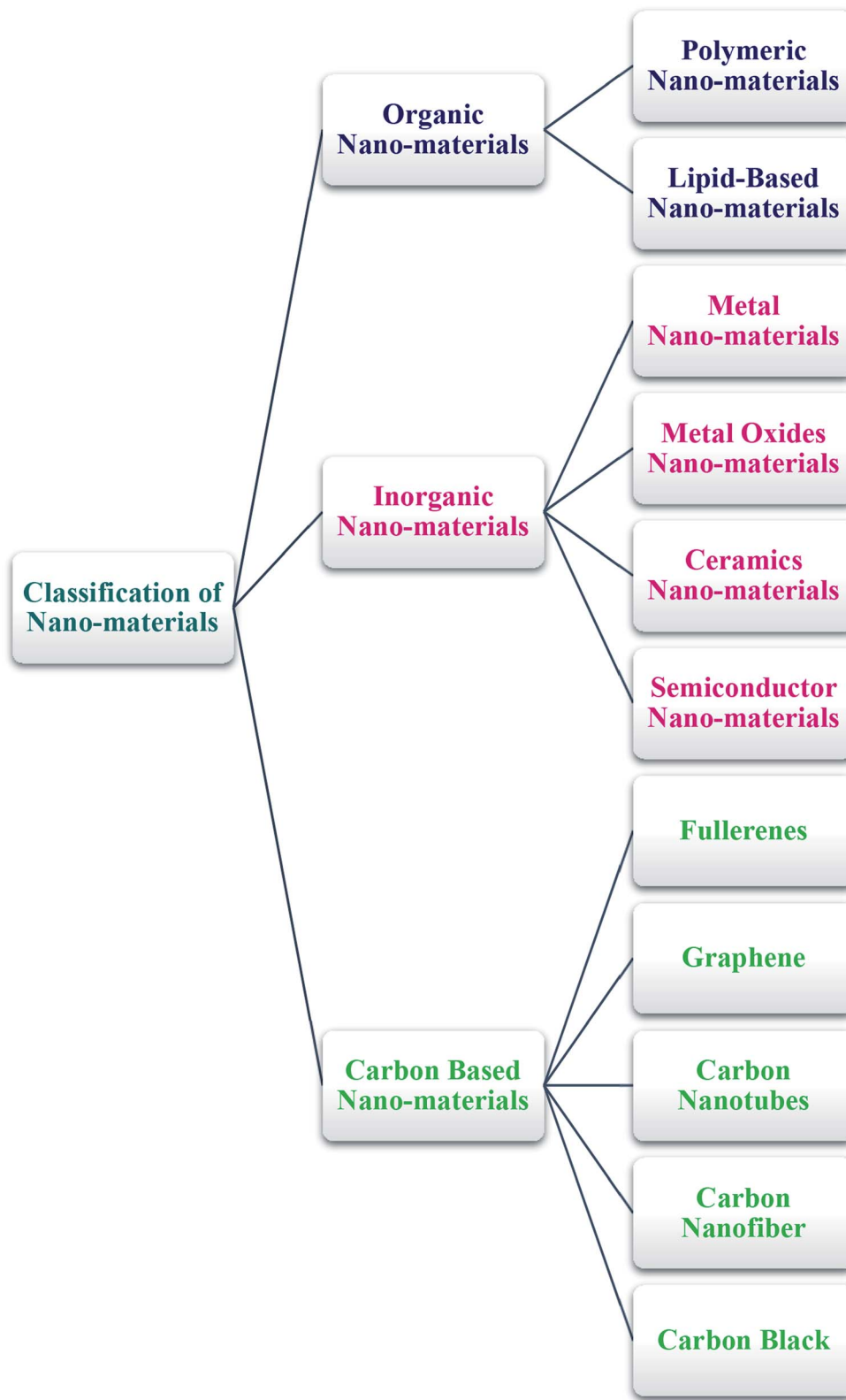
**2.1.1. Polymeric nano-materials.** This category is usually for organic-based nano-materials, which basically have nano-sphere or nano-capsule shapes and can be easily functionalized. Nanospheres are matrix particles with overall solid mass and other molecules are absorbed at the external surface of the spherical surfaces. Nanocapsules are solid mass thoroughly encapsulated into the particle.<sup>36,37</sup>

**2.1.2. Lipid-based nano-materials.** These nano-materials, ranging in diameter in between 10 and 1000 nm, include lipid moieties with effective applications in numerous biomedical fields. Similar to polymeric nano-materials, they possess a solid core, which is made of a lipid and also a matrix containing lipophilic molecules while the emulsifiers or the surfactants stabilize the outer core. They find varied applications in medicine carriers, delivery, and RNA release for treating cancer.<sup>38</sup>

### 2.2. Inorganic nano-materials

Metal and metal oxide-based nano-materials are usually classified under this category.

**2.2.1. Metal nano-materials.** These are completely fabricated from metal precursors. In view of their common localized surface plasmon resonance (LSPR) properties, they enjoy



Scheme 1 General classification of nano-materials.

specific opto-electrical characteristics. Nano-materials of noble metals such as Ag, Au, and Cu and alkali possess a wide adsorption peak in the observable region of the electro-

magnetic solar spectrum; facets, sizes, and shape-monitored metal nano-materials are highly valued as cutting-edge advanced materials.<sup>39-41</sup>



**2.2.2. Metal oxide nano-materials.** Mostly, metal oxide nano-materials are synthesized because of higher reactivity and effectiveness. Some examples are cerium oxide ( $\text{CeO}_2$ ), zinc oxide ( $\text{ZnO}$ ), aluminium oxide ( $\text{Al}_2\text{O}_3$ ), titanium oxide ( $\text{TiO}_2$ ), magnetite ( $\text{Fe}_3\text{O}_4$ ), iron oxide ( $\text{Fe}_2\text{O}_3$ ), and silicon dioxide ( $\text{SiO}_2$ ), which are frequently synthesized oxides. Such nano-materials exhibit exceptional features in comparison to their metal analogues.<sup>42,43</sup>

**2.2.3. Ceramic nano-materials.** These are inorganic non-metallic solids, which are synthesized through heating and consecutive cooling and exist in polycrystalline, dense, amorphous, porous, or hollow forms with applications in catalysis, photo-degradation of dyes, photo-catalysis, and imaging applications.<sup>44,45</sup>

**2.2.4. Semiconductor nano-materials.** Semi-conductor materials have features between metals and non-metals, and because of their broad bandgaps, their features are significantly altered as the bandgaps are tuned. Thus, they are highly prominent materials in photo-catalysis, photo optics, and electronic devices.<sup>46</sup>

### 2.3. Carbon based nano-materials

Carbon-based nano-materials can be grouped into fullerenes, graphene, carbon nanotubes, carbon nanofibers, carbon black, and occasionally, actuated carbon with nanometer size.<sup>47</sup>

**2.3.1. Fullerenes.** Fullerene ( $\text{C}_{60}$ ) is a spherical carbon molecule made up of carbon atoms, which are bonded to each other *via*  $\text{sp}^2$  hybridization with nearly 28 to 1500 carbon atoms, comprising spherical structures with a diameter of 8.2 nm for each layer and 4 to 36 nm for the multilayers.<sup>48</sup>

**2.3.2. Graphene.** Graphene is one of the allotropes of carbon. It has a hexagonal network with a honeycomb lattice consisting of carbon atoms in a 2D planar surface. In general, the thickness of a graphene sheet is  $\sim 1$  nm.<sup>49,50</sup>

**2.3.3. Carbon nanotubes.** Carbon nanotubes are graphene nano-foils with a honeycomb lattice of carbon atoms, which are twisted in an empty cylinder, forming nano-tubes that are as small as 0.7 nm for a one-layered carbon nanotube and 100 nm for the multilayered carbon nanotubes, which varies from a few micro-meters to many millimeters. The end of nanotubes may be unfilled or closed *via* a half fullerene molecule.<sup>51-53</sup>

**2.3.4. Carbon nanofiber.** Similar to graphene, nano-foils are employed for producing carbon nano-fiber as carbon nanotubes but they are twisted into a cup- or cone-shape rather than a conventional cylindrical tube.<sup>54</sup>

**2.3.5. Carbon black.** It is an unshaped carbon object that is usually spherical in shape with a diameter in the range of 20 to 70 nm. The particles have a great interaction that leads to binding of the aggregates so that approximately 500 nm-sized agglomerates are established.<sup>55</sup>

## 3. Synthesis of nano-materials

Two main techniques are deployed for the synthesis of nano-materials and are broadly classified into top-down and bottom-up methods (Scheme 2).

### 3.1. Top-down synthesis

Destructive or top down technique refers to the decrease in bulk materials to the nano-meter scale particles with mechanical milling, sputtering, nano-lithography, laser ablation, and thermal decomposition as the synthetic techniques with widespread applications.

**3.1.1. Mechanical milling.** Amongst different top down techniques, mechanical milling is one of the widely used methods for generating different nano-particles and is applied to mill and post-anneal nanoparticles during syntheses, in which various components are milled. Plastic deformation is a parameter affecting the mechanical milling, which results in the particle shape and fracturing, resulting in the decrease in particle sizes, and cold-welding, leading to an increase in the particle size.<sup>56-58</sup>

**3.1.2. Nano-lithography.** Studying the fabrication of nano-meter scale structures with at least one dimension in the size ranging between 1 and 100 nm is termed as nano-lithography with different varieties of the nano-imprint, namely, optical, multi-photon, scanning probe lithography, and electron beam.<sup>59,60</sup> In general, lithography refers to the procedure of printing the intended form or structure on light sensitive materials, which eliminates a part of the materials for creating the intended shape and structure in a selective manner.<sup>61</sup>

**3.1.3. Laser ablation.** One of the popular methods for producing nano-materials in different solvents is laser ablation synthesis, which entails the irradiation of a metal immersed in a liquid solution *via* a laser beam that condenses a plasma plume, thus generating the nano-materials.<sup>62</sup>

**3.1.4. Sputtering.** NPs deposition on the surface *via* ejection of particles from it through collision with the ions is called sputtering.<sup>20</sup> It is generally the deposition of a thin layer of NPs accompanied by annealing. The NPs' sizes and shapes are specified by the layer thickness, annealing period, and temperature and type of the substrate.<sup>63</sup>

**3.1.5. Thermal decomposition.** Thermal decomposition process refers to the chemical decomposition through heating, which is endothermic and breaks down the chemical bonds in the compounds. Nano-materials are generated *via* decomposition of the metal at certain temperatures that undergo a chemical reaction, thus generating secondary products.<sup>64,65</sup>

### 3.2. Bottom-up synthesis

Generating materials from atoms to clusters to nano-materials is called bottom-up or constructive technique with widespread applications for producing nano-materials *via* chemical vapor deposition (CVD), sol-gel, spinning, pyrolysis, and bio-synthesis.

**3.2.1. Sol-gel.** One of the widespread bottom-up methods is the sol-gel method because of its straightforwardness. Sol-gel is a wet-chemical procedure with a chemical solution, which is a precursor for discrete particles. Metal oxide and chloride are two precursors that are usually deployed in the sol-gel procedure.<sup>66-69</sup> Afterwards, the precursors are scattered in a host liquid by stirring, shaking, or sonicating. The final system comprises a solid and a liquid phase. A separated phase is



Scheme 2 Conventional synthetic techniques for nano-materials.

applied for recovering the nano-materials *via* different techniques, including sedimentation, filtration, and centrifugation. Moisture is often additionally eliminated *via* drying.<sup>70,71</sup>

**3.2.2. Spinning.** Spinning disc reactor (SDR) has been used to synthesize nano-materials *via* spinning, which involves a spinning disc within a reactor/chamber, in which physical variables including temperature may be monitored. In general, nitrogen or other inert gases are filled in the reactor to remove oxygen and to avoid chemical reaction. The disc spins at various velocities, in which the solution with water and precursor are pumped in. The spinning process results in the fusion of molecules or atoms, which is followed by precipitation, collection, and drying. The properties of the nano-materials synthesized from SDR are determined by distinct operational variables such as disc surfaces, disc rotation velocity, liquid flow rate, liquid or precursor ratio, and feed location.<sup>72-76</sup>

**3.2.3. Chemical vapor deposition (CVD).** CVD refers to the deposition of a thin layer of gaseous reactants over a substrate. The sedimentation process is performed at the ambient temperature in a reaction chamber *via* the combination of gas molecules wherein chemical reaction takes place when a heated substrate

communicates with the fused gas.<sup>8</sup> The reaction results in the formation of a thin layer of product on the substrate surface, which is recyclable and reusable. The temperature of the substrate is one of the factors affecting CVD. The benefits of CVD include higher purity, uniformity, and hardness, with the shortcoming that it requires specific instruments and gaseous by-products that would be strongly poisonous.<sup>77,78</sup>

**3.2.4. Pyrolysis.** Pyrolysis, the burning of a precursor with a flame is a procedure with widespread application in industries with large-scale production of NPs. The vapor or liquid form of the precursor is fed into the furnace with a high pressure through a little orifice for combustion.<sup>79</sup> Afterwards, the combustion or by-product gases are categorized for recovering the nano-materials. A number of furnaces employ laser and plasma rather than flame for producing high temperatures for simple evaporation.<sup>80,81</sup> Pyrolysis enjoys benefits such as simplicity, efficiency, affordability, and continual procedure with great yields.

**3.2.5. Bio-synthesis.** Bio-synthesis refers to a green and eco-friendly strategy for synthesizing nano-materials, which is relatively less toxic and with the possible use of biodegradable



materials.<sup>15</sup> It deploys bacteria, plant extracts, fungi, and enzymes accompanied by precursors for generating nanoparticles rather than traditional chemicals for bio-reduction and capping purposes. The bio-synthesized nano-materials have certain improved biocompatibility features that are useful for bio-medical applications.<sup>82</sup>

## 4. Nano-materials features

In general, nano-material features are classified into physical and chemical features.

### 4.1. Physical features

Physical features involve optical characteristics, including nano-material color, light penetration, adsorption and reflection abilities, UV adsorption, and reflection capability in a solution or coated over a surface. Moreover, it involves mechanical features, including elasticity, ductility, tensile strength, and flexibility, which contribute significantly to their application. Notably, several contemporary industries use other features such as hydrophilicity, hydrophobicity, suspension, diffusion, and settling properties. Electrical and magnetic features, including conductivity, semiconductivity, and resistivity, provide the grounds for using nano-materials in contemporary electronics, thermal conductivity, and renewable energy applications.<sup>83,84</sup>

### 4.2. Chemical characteristics

Chemical characteristics pertain to reactivity of the nano-materials with the target, stability, and sensitivity to variables such as atmosphere, humidity, light, and heat that determines the applications of nano-materials. Anti-bacterial, antifungal, disinfection, and toxicity are perfect nano-material features for biomedical and environmental uses. Corrosive, anti-corrosive, oxidation, decline, and flammability properties of nano-materials determine their applications.<sup>85,86</sup>

## 5. Characterizing nano-materials

Various characterization methods have been developed to analyze different physico-chemical features of nano-materials, namely, scanning electron microscopy (SEM), X-ray diffraction (XRD), infrared spectroscopy (IR), transmission electron microscopy (TEM), X-ray photo-electron spectroscopy (XPS), and Brunauer–Emmett–Teller (BET) and particle size analyses.

### 5.1. Morphological properties

The morphological properties of nano-materials have been consistently and greatly considered because morphology invariably affects a majority of the nano-material's features. Various characterization methods have been proposed for morphological examinations; however, microscopic methods, including SEM, polarized optical microscopy (POM), and TEM are the most prominent techniques. SEM is based on the electron scanning principle, which presents information about the materials at the nano-scale levels.<sup>87</sup>

### 5.2. Structural features

Structural features are crucial for studying the compositions and nature of the binding materials. XRD, EDX, XPS, Raman, IR, BET, and zeta potential and size analysis are the prevalent methods employed for studying the structural features of nano-materials.<sup>88</sup>

### 5.3. Particle size and surface area

It is possible to use various procedures for estimating the size of the nano-materials such as TEM, XRD, and SEM, although the zeta potential and size analysis by dynamic light scattering (DLS) may be applied for finding the sizes of extremely small nano-materials.<sup>89</sup>

### 5.4. Optical features

The optical features are crucial in photo-catalytic applications and the knowledge of the mechanisms can be exploited for photo-chemical procedures. Such features are according to the popular Beer–Lambert's law and the fundamental principles of light. Such methods provide knowledge of the luminescence, adsorption, reflectance, and phosphorescence features of the nano-materials.<sup>90</sup>

## 6. Dental applications of nano-materials

Injured dental tissues may result in dental caries, periodontal diseases, tooth sensitivity, unpleasant breath, and oral pre-cancerous and cancerous conditions. All of the above complications may be treated *via* therapeutic interventions and application of bio-compatible synthetic materials. Nanomedicines applied as dental materials possess certain physico-chemical and biological features, which make them superior for overcoming the side effects related to more conventional dental therapies.<sup>91</sup> Research has shown that various kinds of nano-materials mimic the host tissue features,<sup>92,93</sup> though the knowledge of such features amongst dental communities is not available. Hence, the present review focuses on the characteristics of various metal and polymer-based nano-materials employed in adhesive and restorative dentistry, acrylic resins, periodontology, tissue engineering, endodontics, and implant dentistry.<sup>94–96</sup>

### 6.1. Nano-materials for preventive dentistry

Teeth function in the dynamic environment of the oral cavity, wherein it is a big challenge to prevent tooth decay. Because of the accumulated knowledge-base on oral diseases, preventive dentistry is imperative and plays a significant role. Nano-materials are employed in preventive dentistry, managing biofilms at the surface of teeth through nano-apatites, and demineralizing the initial stage of submicron-sized enamel lesions.<sup>97,98</sup>

Schwass *et al.* designed a silver NP (Ag NP) formulation as a targeted application for disinfecting carious dentine. Sodium borohydride ( $\text{NaBH}_4$ ) decreased silver nitrate ( $\text{AgNO}_3$ )



chemically in the presence of sodium dodecyl sulfate (SDS) to form micelle aggregate structures with mono-dispersed stabilized Ag NPs with size in the range of 6.7 to 9.2 nm. On triplicate testing of Ag NPs against *Streptococcus gordonii* DL1, C219, G102, and ATCC10558 strains, *Streptococcus mutans* UA159, *Streptococcus mitis* I18, and *Enterococcus faecalis* JH22 for planktonic bacteria, the minimum suppressive concentrations were determined to be as low as 7.6  $\mu\text{g mL}^{-1}$  with the lowest bactericidal silver concentration of 19.2  $\mu\text{g mL}^{-1}$ . Microplate readings, which detect crystal violet light adsorption at 590 nm, exhibited considerable difference among the Ag NP treated biofilms. The presence of sucrose had no effect on the sensitivity of bacteria. During the prevention of *in vitro* bio-film creation for numerous *Streptococcus* spp. and *Enterococcus faecalis*, this Ag NP formulation showed potential for clinical applications in suppressing bio-films.<sup>99</sup>

Favretto *et al.* conducted a study to evaluate the capability of fluoride toothpastes (1100 ppm F), which contain sodium trimetaphosphate (TMP) NPs, in enhancing the obliteration of dentinal tubules with or without acid challenges. They intended to confirm if the reduction in the size of sodium trimetaphosphate NPs could additionally increase these impacts or not. Sodium trimetaphosphate NPs enriched fluoride toothpastes enjoy the same capability for occluding dentinal tubules as a toothpaste with 1100 ppm F, in which an acidic situation could not change the obliterating dentinal canals and the particle sizes did not affect the outputs. When sodium trimetaphosphate NPs have been added, fluoride toothpastes can

occlude the dentinal canals with a capacity for reducing dentin hypersensitivity.<sup>100</sup>

Manikandan *et al.* explored the formation of silver oxide NPs ( $\text{Ag}_2\text{O}$  NPs) via *Ficus benghalensis* prop root extract (FBPRE) as a stabilizing and decreasing agent and assessed its anti-bacterial activities *versus* dental bacterial strains; higher extract concentrations and time frame have been observed with a considerable enhancement in the formation of NPs. The FBPRE and  $\text{Ag}_2\text{O}$  NPs combination has been found to display very good anti-bacterial activity against both dental bacteria *Lactobacilli* sp and *Streptococcus mutans*. Their outcome indicated that blending the synthesized FBPRE and  $\text{Ag}_2\text{O}$  NPs would be beneficial as a germicidal factor in toothpastes after several studies on animal models.<sup>101</sup>

Mackevica *et al.* examined the release of Ag NP from commercial toothbrushes for children and adults by analyzing the total Ag released and quantifying the particulate Ag NP release. Experimental findings revealed the possible release of Ag NPs from the toothbrushes in the market that might result in potential consumer oral and environmental exposures. Testing these 2 toothbrushes found in the market showed that adult toothbrushes have relatively greater Ag release with regard to the Ag and Ag NP releases. The overall procedure is as follows: release of the particles considerably decreased after six minutes of testing for the first time and the release of total Ag reached a plateau after testing for 16 hours. The median particle size (43–47 nm) was identical for each toothbrush tested. Total Ag release for the two toothbrush brands was at  $\text{ng L}^{-1}$  levels,

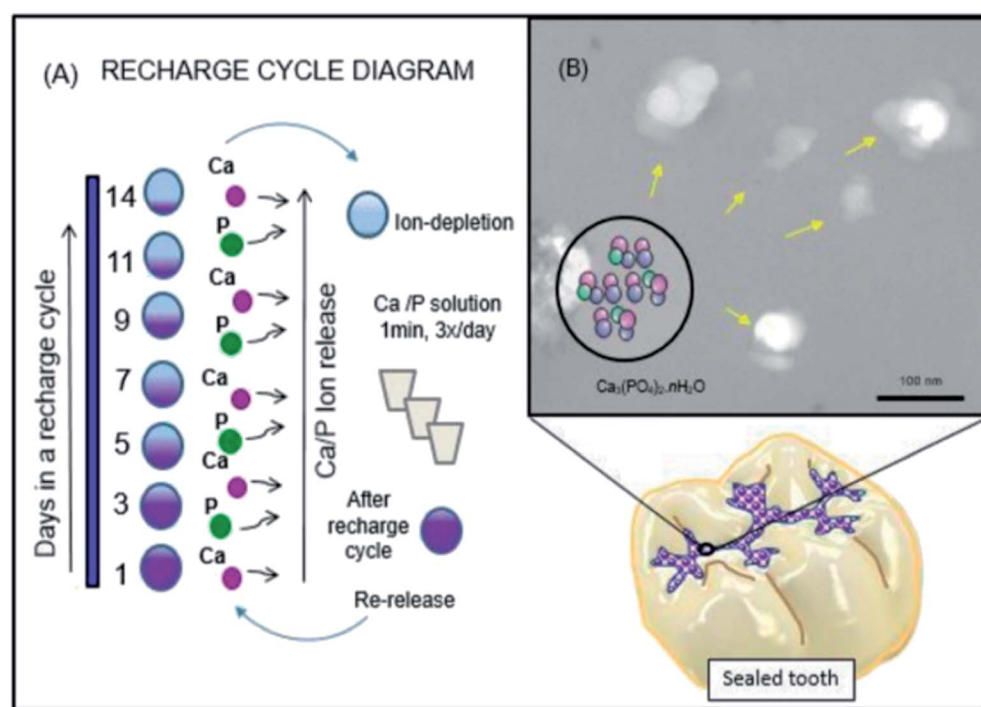


Fig. 2 Schematic diagram of the rechargeable nanoparticles of the amorphous calcium phosphate (NACP) sealant approach to deal with enamel demineralization around the dental sealants: In (A), the recharge cycle diagram illustrates the re-release from the exhausted and recharged NACP sealants. Three recharge/re-release cycles were performed and each re-release was measured for 14 days. The ion re-release increased on increasing the NACP filler level. In (B), the TEM image of NACP from the spray-drying technique, having sizes of about 100–300 nm.<sup>103</sup>



which affirms that there is minor environmental and human exposure from the toothbrushes; however, the safe levels of Ag NP exposure is still unanswered.<sup>102</sup>

Salem Ibrahim *et al.* designed novel anti-bacterial resin-based sealants including NPs of amorphous calcium phosphate (NACP) for  $\text{PO}_4$  and Ca ion release and re-charge characteristics (Fig. 2). They aimed at incorporating various mass fractions of NACP into the parental re-chargeable anti-bacterial sealant, determining the impacts on the mechanical functions, and evaluating the method of studying the effect of the changes in the NACP concentrations on phosphate ( $\text{PO}_4$ ) and calcium (Ca) ions' release and recharge ability over time. It appears that the addition of an enhanced percentage of NACP had satisfactory physical and mechanical functions, while generating considerable initial ion release and a lengthy iterated recharge ability.<sup>103</sup>

Wassel and Khattab proposed that applying the naturally-occurring products experimentally may be an efficient strategy to prevent caries; Varnish is a mix of natural products with optimum concentrations of fluoride in chitosan NPs (CS-NPs) and potential for ion release, re-mineralization potential, and clinical efficacy. The procured dental varnishes with miswak, propolis, and CS-NPs with or without sodium fluoride (NaF) have been evaluated in terms of the anti-bacterial effects against *Streptococcus mutans* employed in the disk diffusion test. The protecting effects of a single pre-treatment of the main teeth enamel species against *in vitro* bacteria-induced enamel demineralization were evaluated for three days. Each natural product with the varnish largely suppressed the growing bacteria more than that by 5% NaF varnish; however, NaF loaded CS-NPs (CSF-NPs) had maximum anti-bacterial impact, even though there was no significant difference between them and other varnishes with the exception of miswak ethanolic extract varnish. Increased suppressive impact was observed for the varnish with freeze-dried aqueous extract of miswak in comparison to the varnish with ethanolic extract of miswak, which may be caused by the anti-microbial substance concentrations *via* freeze-drying. Adding natural ingredients to NaF in a dental varnish presented additional effects, particularly in comparison with fluoride with varnish; 5% NaF varnish had the most acceptable suppression of the de-mineralization impact. Fluoride with miswak varnish and CSF-NPs varnish considerably suppressed the de-mineralization more favorably than each experimental varnish, although the CSF-NPs varnish exhibited a small fluoride concentration, which may be caused by the more acceptable existence of fluoride ions and more small-sized NPs. One of the most efficient approaches to prevent caries, in particular, miswak and propolis in a case of limited financial resources, is the incorporation of natural products with fluoride into the dental varnishes.<sup>104</sup>

Nguyen *et al.* conducted a study to develop fluoride loaded NPs on the basis of bio-polymers chitosan, alginate, and pectin for use in dental delivery; polymer-based nano-particulate formulations were developed for providing and improving an instrument for the effective topical delivery of fluoride. In the presence of NaF and a suitable cross-linker, simply chitosan could create stable mono-dispersed NPs. Alginate failed to

create NPs because the optimum ionic strength was greater at the experimented salt concentrations, while pectin produced large undefined nanostructures. It was shown that fluoride loading and the entrapment efficacy of chitosan NPs is 33–113 and 3.6–6.2% ppm, respectively, under the testing conditions. It is possible to optimize the aforementioned values for preparing the variables during the process of incorporating fluoride. Apparently, the release of fluoride increased in an acidic environment while simulating a cariogenic attack. Such features may be largely beneficial for dental formulations, which target patients with high risk of development.<sup>105</sup>

Fathima *et al.* dealt with the synthesis of  $\text{ZrO}_2$  NPs with a crystalline nature and sizes between 15 and 21 nm, as verified *via* SEM, XRD, and TEM analyses. The anti-microbial activities of  $\text{ZrO}_2$  NPs *versus* Gram-positive and Gram-negative bacteria demonstrated the possible suppressive actions of  $\text{ZrO}_2$  NPs against Gram-negative ones, in particular, *Pseudomonas aeruginosa* at greater concentrations because of the respective cell surfaces with negative charges. Therefore, researchers have illustrated the feasibility of exploitation of  $\text{ZrO}_2$  NPs in avoiding tooth decay by analyzing the tooth decay pathways.  $\text{ZrO}_2$  NPs have been suggested for applications in dental care and related bio-medical uses for future *in vitro* and *in vivo* research.<sup>106</sup>

Wang *et al.* exploited carboxymethyl chitosan (CMC) conjugated with alendronate (ALN) for stabilizing amorphous calcium phosphate (ACP) in the formation of CMC/ACP NPs. Sodium hypochlorite (NaClO) served as a protease decomposing amelogenin *in vivo* for degrading the CMC-ALN matrix and generating HAP@ACP core-shell NPs. HAP@ACP NPs were altered by 10 mM glycine, as they were modified from an amorphous phase into well-ordered rod-shape apatite crystals for achieving oriented and ordered bio-mimetic re-mineralization on acid-etched enamel surfaces. The oriented bond of the NPs on the basis of the non-classical crystallization theory contributes to the bio-mimetic re-mineralization procedure. Researchers showed that one of the efficient approaches to remineralize the enamel is to find and develop analogues of natural proteins, including amelogenin engaged in bio-mineralization *via* natural macro-molecular polymers and imitation of the biomineralization procedure. The above technique could be a potential procedure for managing the initial caries in minimal invasive dentistry.<sup>107</sup>

Liu *et al.* demonstrated the ability of ferumoxytol to disrupt the intractable oral bio-films and prevention of tooth decay (dental caries) through intrinsic peroxidase-like activities. Ferumoxytol binds to the bio-film ultra-structure and produces free radicals from hydrogen peroxide ( $\text{H}_2\text{O}_2$ ), which causes *in situ* bacterial mortality through cell membrane disruptions and degradation of the extra-cellular polymeric substance matrix. When combined with a small concentration of  $\text{H}_2\text{O}_2$ , ferumoxytol suppressed the bio-film stacked on natural teeth in a human extracted *ex vivo* biofilm model and stopped acid injury of the mineralized tissues. Developing dental caries *in vivo* is suppressed by topical oral therapy with  $\text{H}_2\text{O}_2$  and ferumoxytol, and prevents the initiation of serious tooth decay (cavity) in a rodent model of the disease. Histological and microbiome analysis did not present any consequences on the



oral microbiota diversities and gingival and mucosal tissues. Researchers have found a novel bio-medical application for ferumoxytol as a topical therapy for the common and prevalent bio-film, which results in oral diseases.<sup>108</sup>

A bio-nanocomposite of Carboxymethyl Starch (CMS)-Chitosan (CS)-Montmorillonite (MMT) has been designed to deliver Curcumin (Jahanzadeh *et al.*). They used ionic gelation technique and examined its anti-biofilm activities *versus* *Streptococcus mutans*. Various formulations have been designed by response surface technique for obtaining the optimum composition with maximum medicine loading and minimum particle sizes; entrapment efficacy and particles size were influenced by MMT amounts, surfactant concentrations, and poly-saccharide concentrations. The results from the bacterial culture on the dental model demonstrated the powerful biofilm reduction impact of the nano-composite with curcumin.<sup>109</sup>

Al Dulaijan *et al.* used Menschutkin reaction to synthesize dimethyl-aminohexadecyl methacrylate (DMAHDM). A spray-drying method was applied to synthesize NPs of amorphous calcium phosphate (NACP). Resin included ethoxylated bisphenol A dimethacrylate (EBPADMA) and pyromellitic glycerol dimethacrylate (PMGDM) and re-chargeable NACP and rechargeable NACP-DMAHDM were the two constructed composites; ion release, mechanical features, and recharge were evaluated. The bio-film model of dental plaque microcosm was experimented by using saliva. There was a match between the modulus and commercial control composite and flexural strength of rechargeable NACP and NACP-DMAHDM composites ( $p > 0.1$ ). Bio-film metabolic events and lactic acid were suppressed by NACP-DMAHDM, which declined the colony-forming units of the biofilm (CFU) by 3–4 log. NACP and NACP-DMAHDM exhibited identical P and Ca ions' re-charge and re-release ( $p > 0.1$ ). Hence, the addition of DMAHDM did not lead to compromise in the ion re-chargeability; continuous release was induced by 1 re-charge for 56 days and it was kept at a similar level when the number of recharge cycles were enhanced, thus indicating the lengthy ion releases and remineralization ability. Researchers designed the 1st CaP rechargeable and anti-bacterial composite. The addition of DMAHDM to the re-chargeable NACP composite had no adverse effect on the release and recharge of Ca and P ions, and the composite experienced highly lower bio-film growth, lactic acid generation, and CFU decline by 3–4 log.<sup>110</sup>

Yan *et al.* synthesized mesoporous silica NPs (pMSN) for encapsulating chlorhexidine (CHX) as a classic anti-microbial agent. They used CHX@pMSN for modifying traditional dental glass ionomer cement (GIC) for the first time. It was revealed that CHX@pMSN modified GIC at 1% (w/w) could attain the sustained release of CHX and effective inhibition of the formation of *Streptococcus mutans* biofilm with no impact on the mechanical features of GIC. The findings disclosed that addition of 1% (w/w) CHX@pMSN into the GIC had significant potential as a novel approach *versus* secondary caries, which prolonged the conventional GIC service life. In addition, the enduring effects of incorporating CHX@pMSN into GIC have to be assessed in more complicated scenarios *via* artificial aging methods, for example, pH cycling, sodium hypochlorite

treatment, and lengthy storage. However, it is necessary that further research should deal with more favorable incorporation approaches for endowing GIC with influential anti-microbial capability and higher mechanical functions.<sup>111</sup>

Maghsoudi *et al.* examined the anti-biofilm activity of nano-sized curcumin-loaded particles synthesized by desolvation technique. Nano-particle systems have been explored in terms of the properties against *Streptococcus mutans* functions on dental models when curcumin was applied as a biological anti-bacterial factor to load into NPs. The findings determined the size of the generated NPs with chitosan, starch, and alginate to be 61.1, 66.3, and 78.8 nm, respectively; the corresponding zeta potential were  $-14.7$ ,  $+21.7$ , and  $-23.4$  mV, respectively. The highest amount of curcumin loaded onto the NPs was for chitosan (51.03); however, it was 24.59 and 29.69 for starch and alginate, respectively. It was estimated that the lowest suppressive concentration (MIC) was  $0.114\text{ mg mL}^{-1}$  for chitosan NPs while alginate and starch NPs had a MIC of  $0.204\text{ mg mL}^{-1}$ . Analyzing the release showed burst release after 96 hours for chitosan and 48 hours for alginate; the release amounts were 92.8% and 51.4%, respectively, while the starch NPs exhibited a release with higher stability. When the equilibrium point reached the end of 122 hours, the release of 81.6% of curcumin was observed. Moreover, the impacts of curcumin-loaded NPs on *Streptococcus mutans* bio-films were evaluated for the dental models. These findings indicate that curcumin-loaded chitosan NPs could be applied in dental decay fighting products.<sup>112</sup>

Covarrubias *et al.* designed a study to develop hybrid NPs (CuCh NP) containing copper NPs with a chitosan shell. Anti-microbial features of CuCh NP have been evaluated against *Streptococcus mutans*, which is a major bacterium causing tooth decay and their activities could be compared to the oral anti-microbial agents, including cetylpyridinium chloride and chlorhexidine. In particular, CuCh NP exhibited greater capacities for preventing the growth of *Streptococcus mutans* on the human tooth surface, disrupting and killing the bacterial cells in the formed dental biofilm. It is possible that there is an interaction between the chitosan and tooth hydroxyapatite and the bacterial cell wall, which enhances copper adherence to the tooth surface and increased their antibiofilm actions. The anti-microbial features of CuCh NP may be advantageous for the development of more efficient therapies to control dental plaque biofilms.<sup>113</sup>

Gitipour *et al.* dealt with developing a nano-silver disinfectant (ASAP-AGX-32, an anti-microbial cleaner for dental units, 0.0032% Ag) and a bio-film. The researchers assembled an in-house dental unit water lines (DUWL) model for simulating the disinfection scenario so that the grounds for accumulating the biofilm were provided. Gitipour *et al.* found that absorbing Ag NPs on the bio-film surfaces could be helpful in illustrating the toxicity mechanism of Ag NPs on the biofilm and bacteria. Therefore, this study might be an initial step in gaining more knowledge as to how Ag NP transformation is dependent on the exposed conditions during their lifetime. So far, a majority of the studies have considered the assessment of the effects of pristine (lab synthesized) nano-materials on different systems.<sup>114</sup>



Ionescu *et al.* assessed bio-film formation and bacterial adhesion on resin-based composites (RBC) such as dicalcium phosphate dihydrate NPs (nDCPD) wherein they illustrated anti-adherent or anti-biofilm activity of nDCPD-filled RBC. Functionalizing nDCPD declined the surface roughness of RBCs, which contributed to the decrease in biofilm formation and adherence on the material surfaces. Therefore, an optimal formulation of the bio-mimetic RBCs would be as crucial as the bio-mimetic active principle alone in the regulation of micro-biological behaviors, which probably prevents the development of secondary caries.<sup>115</sup>

## 6.2. Nano-materials for edentulism

Edentulism has serious side effects, including reduced intake of nutritious food and unsatisfactory appearance and has an increased pervasiveness in numerous countries. In spite of the estimates of tooth loss declines, the age group, in which edentulism would still be greatly common, has been getting broader. Therefore, it is strongly necessary for denture therapy in public health, which would enhance with the population's age.<sup>116-118</sup>

Totu *et al.* procured polymethylmethacrylate (PMMA)/titanium dioxide NPs ( $\text{TiO}_2$ ) nano-composites and employed nano-sized  $\text{TiO}_2$  filler synthesized using a modified sol-gel technique;  $\text{TiO}_2$  nanofiller experienced a homogeneous dispersion into the PMMA solution, which was verified by morphological and structural analyses. Experimental data confirmed that the addition of  $\text{TiO}_2$  NPs changed the polymer structure and its certain features; 0.4%  $\text{TiO}_2$  NPs content in the nano-composite largely modified the FTIR spectrum. The incorporation of  $\text{TiO}_2$  NPs in the PMMA polymer matrix provided anti-bacterial impacts, particularly in the *Candida* species, as confirmed by 0.4% nano-composite application *via* stereolithographic method for complete fabrication of the denture.<sup>119</sup>

Rodrigues Magalhães *et al.* described the application of  $\text{TiO}_2$  nano-tubes for enhancing the biological and mechanical features of dental materials. Yttria-stabilized tetragonal zirconia poly-crystals (Y-TZP) have a growing application in dentistry as a substructure for fixed partial prostheses and crowns. Regardless of its optimum clinical outputs, Y-TZP has susceptibility to failures such as micro-structure-associated defectives presented in the fabrication procedure, which could decline its clinical and structural reliability. Researchers assessed the role of the production procedure of the blanks and their original composition modifications *via* the addition of  $\text{TiO}_2$  nano-tubes (0%, 1%, 2%, and 5% in volume) while monitoring each fabrication step. The addition of  $\text{TiO}_2$  nano-tubes in various combinations affected the experimental Y-TZP features and resulted in less flexural strength. Moreover, the nano-tubes resulted in larger grain dimensions, more pores, and a minor enhancement in the mono-clinic phase, which influenced the micro-structure of Y-TZP. Furthermore, the addition of  $\text{TiO}_2$  nano-tubes was accompanied by greater Weibull modulus values and higher structural reliability.<sup>120</sup>

Gad *et al.* determined the effects of addition of zirconium oxide (nano- $\text{ZrO}_2$ ) NPs on the tensile and translucent strength of polymethyl methacrylate (PMMA) denture base material; the tensile strength mean of PMMA in the test groups of 2.5% NZ, 5% NZ, and 7.5% NZ was considerably greater compared to the controls. The tensile strength experienced a significant increase after the addition of nano- $\text{ZrO}_2$  and the highest amount of increase was seen in the 7.5% NZ group. The values of translucency in the experimental group were remarkably less than the values in the controls. In the powered group, 2.5% NZ group showed greater translucency values in comparison with 5% NZ and 7.5% NZ groups. The enhancement in the tensile strength of the denture base acrylic was directly proportional to the nano- $\text{ZrO}_2$  concentration while PMMA translucency declined when nano- $\text{ZrO}_2$  concentration was increased.<sup>121</sup>

Sarraf *et al.* built a hybrid biofunctionalized coating encompassing nano-tubular rows of titanium dioxide ( $\text{TiO}_2$  NTs) with decorated silver oxide NPs ( $\text{Ag}_2\text{O}$  NPs) on their edges in order to improve the biological behaviors and anti-bacterial activities of  $\text{Ti}_6\text{Al}_4\text{V}$  implants (Fig. 3). After making a nano-tubular structure *via* anodization of the substrate,  $\text{Ag}_2\text{O}$  NPs were accumulated on the NTs through physical vapor deposition in 30 s. *In vitro* bioactivity analysis revealed the deposition of apatite on  $\text{Ag}_2\text{O}$  NPs that is decorated on  $\text{TiO}_2$  NTs after soaking in simulated body fluid for a day. After 14 days, the apatite quantity increased significantly with the enhancement in submersion time and led to the formation of a thick layer of apatite with a Ca/P ratio of 1.58. This novel  $\text{Ag}_2\text{O}$  NPs-decorated  $\text{TiO}_2$  NTs had good bactericidal effects against *Escherichia coli* and resulted in 100% eradication within two hours. In addition, osteointegration examinations *via* human osteoblast cells were accompanied by large finger-like protrusions and filopodial activities of the cells, showing their efficient activation by the NT architecture. Moreover, consecutive rapid growth throughout the culture duration was shown by alamar blue assay and confocal laser scanning microscopy observations of the stained human osteoblast cells. Thus, this newly developed  $\text{TiO}_2$  NT coating covered with  $\text{Ag}_2\text{O}$  NPs can efficiently ameliorate the *in vitro* bioactivities of the implant alloys and establish a suitable bactericidal impact with minor cytotoxic responses.<sup>122</sup>

Gunputh *et al.* addressed two strategies for coating  $\text{TiO}_2$  NTs with Ag NPs, which also employed a less dangerous reducing agent,  $\delta$ -gluconolactone. These techniques were suitable for creating Ag NPs with a main particle size  $\sim$ 100 nm; however, an obvious difference was observed in the Ag NP clustering based on the synthetic procedure. The mixing technique resulted in micron clusters of Ag NPs; however, consecutive addition technique resulted in much smaller nanoclusters, which showed anti-bacterial effect on *Staphylococcus aureus*. In addition, the amount of silver released from the coated NPs in the first 24 h was useful for patient healing. The maximum risk of infections was during the few hours immediately after implant operation.<sup>123</sup>

Yang *et al.* revealed feasible coating of dental implants under an extra-corporeal magnetic field with lower concentration of PLGA ( $\text{Ag}-\text{Fe}_3\text{O}_4$ ) for improving the biological compatibility with no effects on the anti-bacterial efficacy (Fig. 4). A



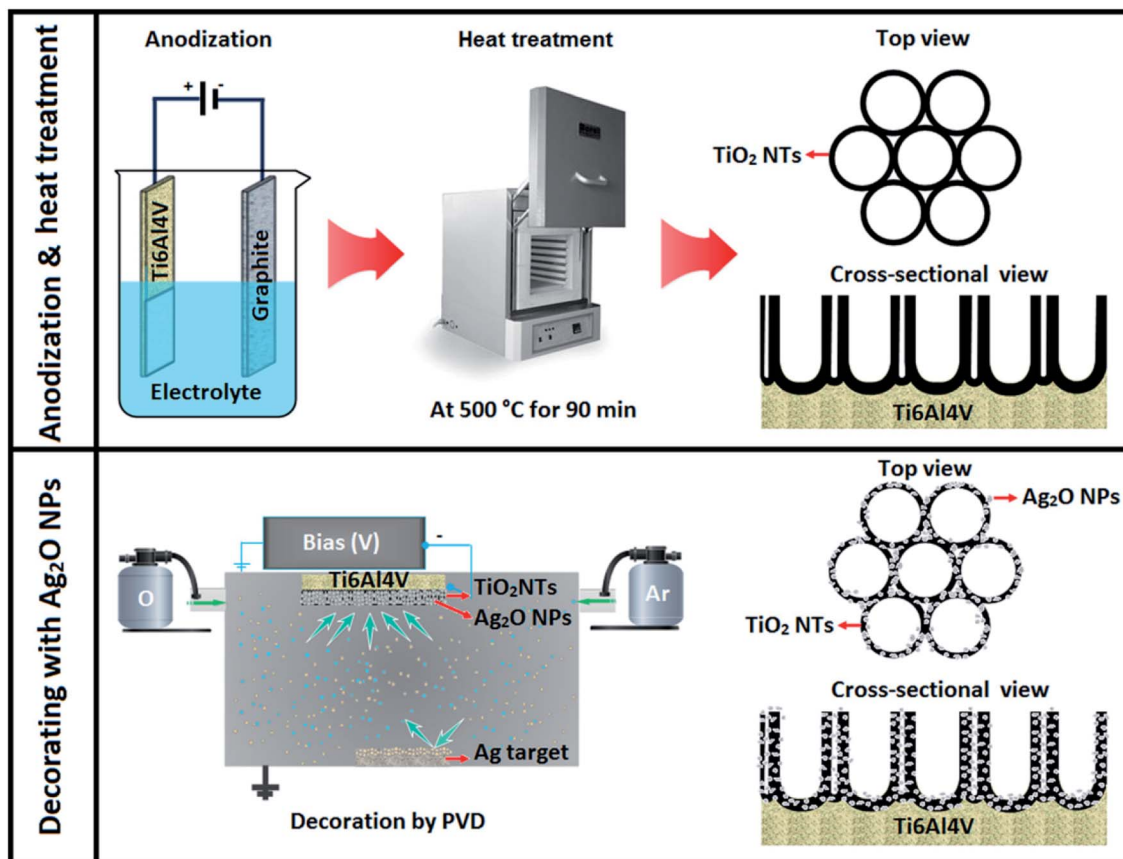


Fig. 3 Schematic representation of the anodization setup and the development of TiO<sub>2</sub> NTs as well as PVD decoration of Ag<sub>2</sub>O NPs on the nanotubular layer.<sup>122</sup>

permanent magnet was applied for building the magnetic field as close to the PLGA (Ag-Fe<sub>3</sub>O<sub>4</sub>) as possible, which was employed *in vivo* to the implanted tooth containing a permanent magnet, thus providing Ag adhesion to the tooth surfaces with no removal *via* flushing water. Bacterial infections, including the infection caused by *Streptococcus mutans*, triggered the host immune responses for producing reactive oxygen species (ROS), which led to the demolition of the tooth supporting tissues (Fig. 4, left). In the implanted tooth coated with PLGA (Ag-Fe<sub>3</sub>O<sub>4</sub>), bacterial adhesion was undermined. Therefore, ROS was not produced by the immune system and the micro-environment surrounding the implanted area triggered osteoblast proliferation, which improved the transplant success rates.<sup>124</sup>

Jang *et al.* proposed bio-compatible Pd-Ag-HAp NPs, which were efficiently deposited onto the extended TiO<sub>2</sub> obstacle layer in a 1.3 M (NH<sub>4</sub>)<sub>2</sub>PO<sub>4</sub> + 0.5 M NH<sub>4</sub>F electrolyte solution. They demonstrated that the protrusion patterns were slowly deposited over the TiO<sub>2</sub> obstacle oxide film and were rough. Abnormal patterns due to Pd-Ag-HAp NPs might obviously be differentiated from the TiO<sub>2</sub> nano-tube oxide layer formed by the anodizing procedure. The element mapping dots usually had a homogeneous distribution throughout the surface of the film. In particular, Pd and Ag had a uniform distribution throughout the surface areas of the protrusion patterns; however, P, Ca, Ti,

and P were remarkably closer to the obstacle surface. The representative protrusion patterns basically comprised Pd-Ag-HAp NPs linked to the TiO<sub>2</sub> obstacle oxide film. Pd, Ag, Ca, P, and Ti were found across the surface areas over the electro-deposited surfaces. Based on the bio-compatibility analyses of the surface, when it was soaked for 20, 23, and 26 days in the SBF solution, the entire surface was coated with HAp precipitate with a turtle-shape crack because of the diffusing ions into the triggered body fluid solution. The Ca/P rate was 1.66, which was nearly identical to the bulk HAp rate. Hence, the protrusion pattern surface contained Pd-Ag-HAp NPs on the TiO<sub>2</sub> obstacle layer, which affected the bio-compatibility.<sup>125</sup>

Rosenbaum examined the effects of copper extracted TiO<sub>2</sub> surfaces (nCu-nT-TiO<sub>2</sub>) on the mortality of *Escherichia coli* and nosocomial *Staphylococcus aureus*. Anodic oxidation of pure titanium sheets in fluorhydric solutions were used to make TiO<sub>2</sub> nano-tube (nT-TiO<sub>2</sub>) arrays, which resulted in surface nano-structuration and the generation of certain reactive locations. Copper nano-cubes with a mean size of 20 nm were synthesized and precipitated on the nT-TiO<sub>2</sub> surfaces through pulsed electro-deposition from a copper sulphate solution. Bacterial examination implied higher biocide potential of the nCu-nT-TiO<sub>2</sub> surfaces, leading to the total mortality of *Staphylococcus aureus* and *Escherichia coli*.<sup>126</sup>

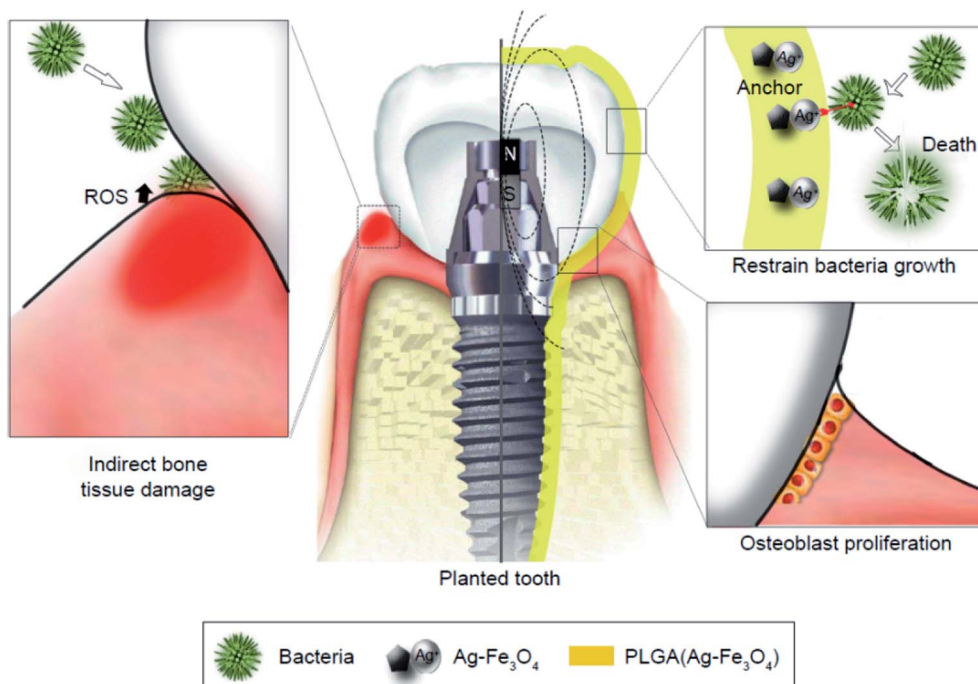


Fig. 4 Schematic diagram of PLGA ( $\text{Ag}-\text{Fe}_3\text{O}_4$ )-coated on dental implants.<sup>124</sup>

Azzawi *et al.* found that the modified laser method is a good procedure for improving the dental implant surface features and the respective osteo-integration. They used titania and nanotechnology where the surface of titanium was exposed to ablation, coating deposition, and heat treatment, concurrently. Nanotitania is considered as a proper substance to coat, roughen, and optimize the bio-compatibility of titanium implant fixtures. In addition, it is possible that this oxide increases the responses of peri-implant bone and accelerates the treatment procedure surrounding the implant fixture. Dip-coating and the modified laser deposition methods affected the production of bio-compatible titania coating with various features such as film thickness, chemical compositions, surface morphologies, crystallinity, pore configurations, and surface roughness, which may have an effect on the bone tissue responses. The modified laser-coated specimens demonstrated more important improvements in the bond strength at the bone-implant interface compared to the dip-coated specimens.<sup>127</sup>

Kim *et al.* presented an easy and effective strategy to build a stable Ag nano-structure on the Ti surface (Fig. 5) using a two-step procedure containing TIPS and Ag sputtering. A nano-structured TIPS-Ti surface offers a nano-template that is mechanically stable, over which an Ag coating was scattered. The nano-structured TIPS-Ti surface ensured that adequate space was created for accepting the Ag stabilization spots. Ag scattering over TIPS-Ti resulted in the formation of Ag nano-clusters merely on the TIPS-Ti nano-structure ridges without significant defects. The adjustment of Ag-sputtering duration stabilized the Ag concentration on the TIPS-Ti surface, which increased from 10 to 120 s linearly. Specifically, the 10Ag-TIPS-

Ti sample provided better anti-bacterial activities against *Staphylococcus aureus* and *Escherichia coli* and did not show any obvious cyto-toxicity towards the fibroblast cells. There is a similarity between the cell morphology bound to the 10Ag-TIPS-Ti specimen and their viability and the polished Ti surface. Therefore, the specimen had acceptably balanced anti-bacterial activities and cellular survival. Kim *et al.* concluded that using stabilized Ag on the TIPS-Ti surface has the capability of improving the general treatment after placing the dental implants and promoting long-term stability of these implants.<sup>128</sup>

Boutinguiza *et al.* developed a technique for producing and depositing silver NPs on a substrate in a single-step procedure. The ablation of Ag foils was conducted in open air *via* laser and an inert gas jet for directing the NPs to the substrate. The NPs contained spherical crystalline silver and silver oxide, which were completely anchored on the Ti substrates and had acceptable anti-bacterial activities against *Lactobacillus salivarius*.<sup>129</sup>

Divakar *et al.* examined the efficiency of Ag conjugated chitosan NPs as a future coating material for titanium dental implants. Bio-active molecule chitosan was derived from *A. flavus* Af09 and conjugated with Ag NPs. The ensuing Ag chitosan NPs had acceptable suppressive impact on the growth of two main dental pathogens, namely, *Porphyromonas gingivalis* and *Streptococcus mutans*. It suppressed the adhesion of the two experimented bacteria, could suppress the formation of biofilm, and suppressed the production of QS in the bacteria. Naturally derived chitosan is popular for its anti-bacterial activities towards a distinct group of bacteria. Any cell cyto-toxicity of the NPs did not indicate their bio-compatibility and the coating of



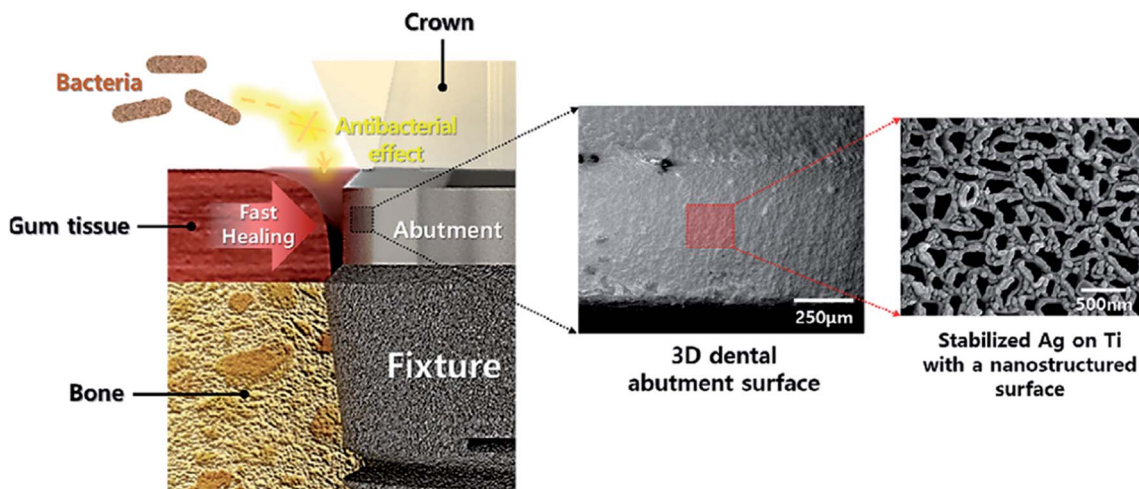


Fig. 5 Antibacterial and bioactive properties of stabilized silver on titanium with a nanostructured surface for dental implants.<sup>128</sup>

titanium dental implants with Ag-chitosan adds the advantage of being corrosion resistant to the dental implants, which enhances the passivating impacts of the implants.<sup>130</sup> Poly(lactic-

*co*-glycolic acid)/Ag/ZnO nano-rods coatings were introduced by Xiang *et al.* over Ti metallic implant surface *via* a hydro-thermal technique and successive spin-coating of the mixture of

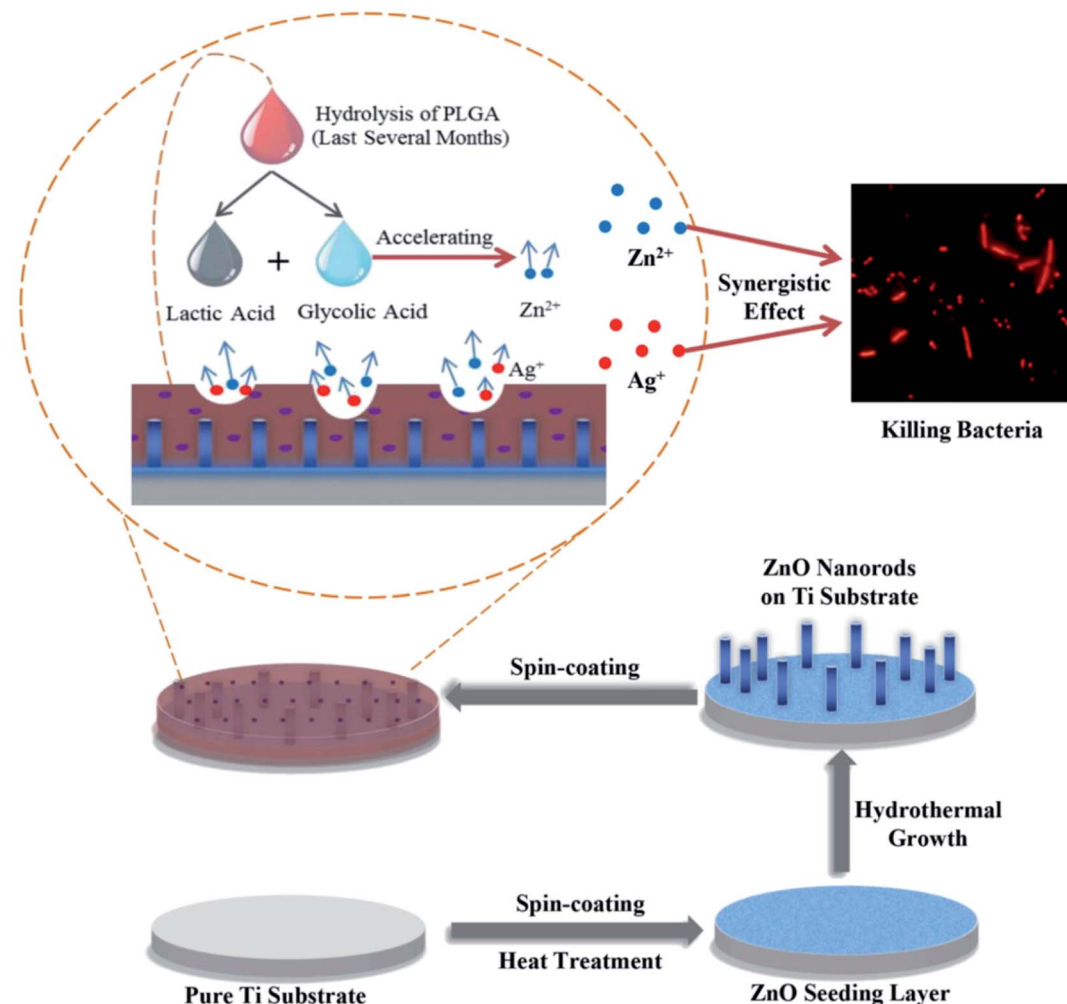


Fig. 6 Schematic illustration of the fabrication process of poly(lactic-co-glycolic acid)/Ag/ZnO nanorods composite coating.<sup>131</sup>



poly(lactic-*co*-glycolic acid) and silver NPs (Fig. 6). Poly(lactic-*co*-glycolic acid)/Ag/ZnO nano-rods coating had very good anti-bacterial efficiency of  $>96\%$  against *Escherichia coli* and *Staphylococcus aureus* while the initial content of Ag NPs was  $>3$  wt%. in addition, the release of silver and zinc was prolonged for  $>100$  days because of the absorption of poly(lactic-*co*-glycolic acid). The rapid growth of mouse calvarial cells showed minimum cyto-toxicity of the poly(lactic-*co*-glycolic acid)/Ag/ZnO coating with an initial Ag NPs content of 1 wt% and 3 wt%, whereas it suppressed the rapid growth of the cells when this value was enhanced to 6 wt%. Finally, this poly(lactic-*co*-glycolic acid)/Ag/ZnO composite might present a lengthy anti-bacterial strategy and acceptable cyto-compatibility, which exhibited remarkable potential for biomedical applications in orthopedic and dental implants with very good self-antibacterial activities and satisfactory bio-compatibility.<sup>131</sup>

Jadhav *et al.* evaluated the osteo-inductive potential of gold NPs (Au NPs) synthesized *via* phyto-chemicals from *Salacia chinensis* (Fig. 7). They confirmed that functionally bio-compatible and stable Au NPs can be successfully synthesized *via* an easy, affordable, and environment-friendly green chemistry technique with applications in bone regeneration. The *in vitro* examinations showed the considerable stability of the gold colloidal dispersion in different blood elements. The researchers indicated that Au NPs are not toxic, as assessed by their cyto-compatibility and blood compatibility with periodontal fibroblasts and erythrocytes. The GNPs showed higher percentage of cell viability ( $138 \pm 27.4$ ) of the MG-63 cell lines in comparison with the controls ( $96 \pm 3.7$ ), indicating their osteo-inductive potential. They found that the bio-compatible and

eco-friendly Au NPs may be applied as efficient bone-inductive adjuvants during implant treatment to form an osteous interface and maintain the emerging peri-implant bone.<sup>132</sup>

### 6.3. Nano-materials for endodontics

The pervasiveness and seriousness of tooth root caries increase with aging from 7% among the young to 56% in seniors with  $\geq 75$  years of age. This is an increasing public health problem because of the fast enhancement in the elderly population as tooth retention enhances in seniors.<sup>14,15</sup> The vulnerability to the root caries may be increased by gingival recession because of aging, periodontal diseases, or traumatic tooth-brushing habits.<sup>133,134</sup> Moreover, small salivary flows in seniors and patients suffering from dry mouth have an additional role in biofilm and plaque formation, and occurrence of root caries. Class V restorations may treat tooth caries. Nonetheless, cleaning and restoration with sub-gingival margins is difficult so that it would augment the developing periodontitis and loss of the tooth's attachment.<sup>135-137</sup> Hence, it is necessary to develop a bio-active Class V composite for eliminating secondary caries and root caries.

Xiao *et al.* performed a study to develop a bio-active multi-functional composite (BMC) through the NPs of amorphous calcium phosphate (NACP), dimethyl-aminohexadecyl methacrylate (DMAHDM), 2-methacryloyloxyethyl phosphorylcholine (MPC), and silver NPs (NAg), and determined the impacts of blended BMC + poly(amido amine) (PAMAM) on remineralizing the demineralized root dentin in a cyclic artificial saliva/lactic acid environment. The mechanical features of BMC were the

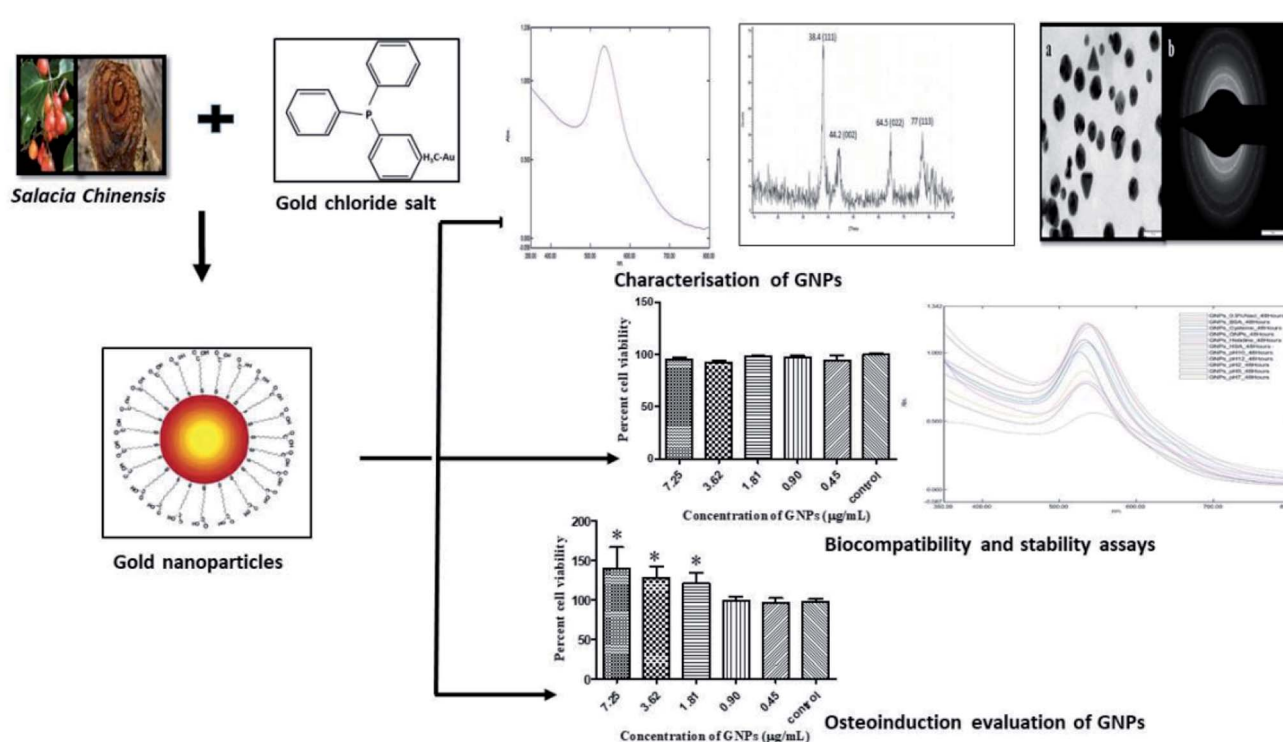


Fig. 7 Phytosynthesis of gold nanoparticles and evaluation of its osteoinductive potential for application in the implant dentistry.<sup>132</sup>



same as that of commercial control composites ( $p = 0.913$ ). BMC possessed very good release of P and Ca ions and acid-neutralization ability. BMC or PAMAM individually obtained minor mineral re-generation in the demineralized root dentin. The blended BMC + PAMAM caused maximum root dentin remineralization and enhanced the hardness of the pre-demineralized root dentin that matched that of the healthy root dentin ( $p = 0.521$ ).<sup>138</sup>

Rodrigues *et al.* assessed the anti-microbial actions of an irritant with silver NPs in an aqueous vehicle, such as sodium hypochlorite, Ag NPs, and chlorhexidine against *Enterococcus faecalis* bio-film and infected dentinal tubules. The Ag NP solution removed little bacteria; however, it could dissolve the biofilm better in comparison to chlorhexidine ( $P < 0.05$ ). NaOCl had maximum anti-microbial activities and biofilm dissolution capacities while the Ag NP solution had lower anti-microbial actions in the infected dentinal canals in comparison to NaOCl ( $P < 0.05$ ). The Ag NP solution highly affected the elimination of planktonic bacteria in dentinal tubules compared to the bio-film after 5 minutes; however, fewer viable bacteria were found in the bio-film in comparison to the intratubular dentine ( $P < 0.05$ ) at 30 minutes. The Ag NP irritant was not as efficient against *Enterococcus faecalis* in comparison with the solutions widely employed in treating root canal. NaOCl is suitable as an irritant as it caused the disruption of the bio-film and elimination of bacteria in bio-films and dentinal canals.<sup>139</sup>

Bukhari *et al.* presented a therapeutic strategy for endodontic disinfections *via* nano-catalysis concept for increasing bacterial destruction across the dentinal tubule. Iron oxide is a sustainable and bio-compatible material, which could be synthesized largely *via* simple and affordable chemical synthetic techniques in view of the current usage in food and drug administration with the verified formulations for chronic treatment. The flexibility in iron oxide chemistry provides the grounds for producing the desired NP shape and size, which can additionally enhance the catalytic activities (probably with less H<sub>2</sub>O<sub>2</sub> concentrations) with higher dentinal tubule penetrations. It is necessary to validate the IO NPs/H<sub>2</sub>O<sub>2</sub> system efficiency by animal models and clinical research, which would result in endodontic therapy with greater effectiveness and efficiency.<sup>140</sup>

#### 6.4. Nano-materials for restoration

Composite resins play vital roles in dental restoration and have several benefits, including acceptable maneuverability, very good esthetics, and satisfactory bio-compatibility.<sup>141–143</sup> The organic elements of the composite resins have been nearly constant over time. The components are mostly methacrylate-type resins such as urethane dimethacrylate (UDMA), bisphenol A-glycidylmethacrylate (Bis-GMA), and triethylene glycol dimethacrylate (TEGDMA).<sup>144</sup> However, several explorations have been conducted on inorganic fillers to develop high-performance composite resins.<sup>145,146</sup> To attain the acceptable lengthy clinical restoration, composite resins should show adequate mechanical features, small polymerization shrinkage, higher wear resistance, and anti-bacterial activities. Therefore,

such necessities can be generally satisfied by using different functionalized fillers.<sup>147,148</sup>

Lee *et al.* strived to develop a hybrid dental resin with Ag NPs for eliminating periodontal diseases resulting from bacteria, including *Streptococcus sobrinus* and *Streptococcus mutans* (Fig. 8). Ag NPs provide the resin with the feature of preventing oral pathogen growth during orthodontic treatment. It has been demonstrated that Ag NPs have experienced a complete synthesis and clear embedding in the dental resin. Regarding the bacterial tests, dental resins with Ag NPs had potential anti-microbial activities against two types of bacteria. Finally, their technique could provide the grounds for generating diverse dental resin and composite products, which could suppress the periodontitis-causing bacteria.<sup>149</sup>

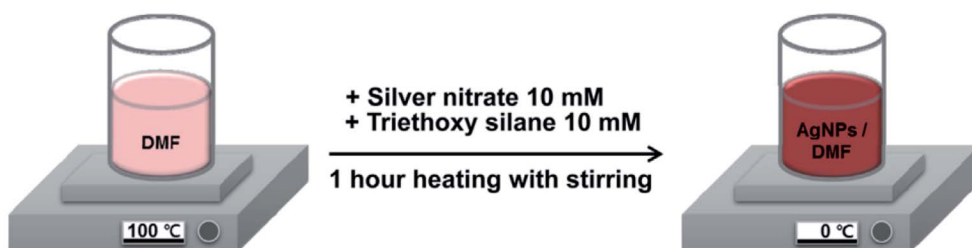
Cao *et al.* described an anti-bacterial nano-composite of silver-loaded polycation functionalized nano-diamonds (Ag/QND) and assimilated them into the dental resin at various proportions for evaluating their effects on the mechanical features, anti-bacterial function, and cyto-toxicity. The outcomes for the mechanical features indicated that the Ag/QND-reinforced composites had greater values of flexural strength, Vickers hardness, and modulus in comparison with pure resins. The resins containing Ag/QND had effective anti-bacterial activities against *Streptococcus mutans*. It was concluded that combined killing impacts of the cationic polymers and Ag<sup>+</sup> could contribute to this scenario. The specimens loaded with  $\leq 1.0$  wt% Ag/QND did not exhibit any considerable cyto-toxicity towards the macrophage cells. Thus, it would be useful to incorporate the newly developed Ag/QND nano-composites to establish a significant improvement in the service-life of resin-based restorative materials.<sup>150</sup>

Cao *et al.*'s study dealt with the development and evaluation of a dental material based on a resin with photo-curable AgBr/BHPVP NPs and they found that the dental resins with AgBr/BHPVP exhibited mechanical properties equivalent to that of the controls. The joint bactericidal impacts of the cationic polymers and Ag<sup>+</sup> ions could contribute to the anti-bacterial activities of the AgBr/BHPVP-incorporated resins. Surprisingly, a concentration of AgBr/BHPVP as low as 1.0 wt% in the dental resins showed adequate and lengthy anti-microbial activities. The specimens with 0.5 and 1.0 wt% AgBr/BHPVP did not show any considerable cyto-toxicity towards the macrophages in comparison with the pure resin disks. Loading the newly developed AgBr/BHPVP nano-composites into the dental resins would be useful for restorations with bacterial and caries suppression for lasting anti-bacterial activities. Moreover, AgBr/BHPVP can have possible advantages on incorporation into other cements, dental adhesives, and sealants for attaining powerful anti-bacterial performance.<sup>151</sup>

Using the sol-gel technique, Zhang *et al.* conducted a study to synthesize Ca-doped mesoporous silica (MCS) NPs and synthesized multifunctional dental resin composites through Ca-doped MCS. The incorporation of Ca-doped MCS into the dental resin led to improvements in the mechanical features of the resin and enabled the dental resin in inducing apatite-mineralization and inhibiting bacterial development. MCS NPs with resin composites could carefully establish responses



## Step I. Synthesis silver nanoparticles in N,N-Dimethylformamide solvent



## Step 2. Preparation of antimicrobial dental orthodontic resin

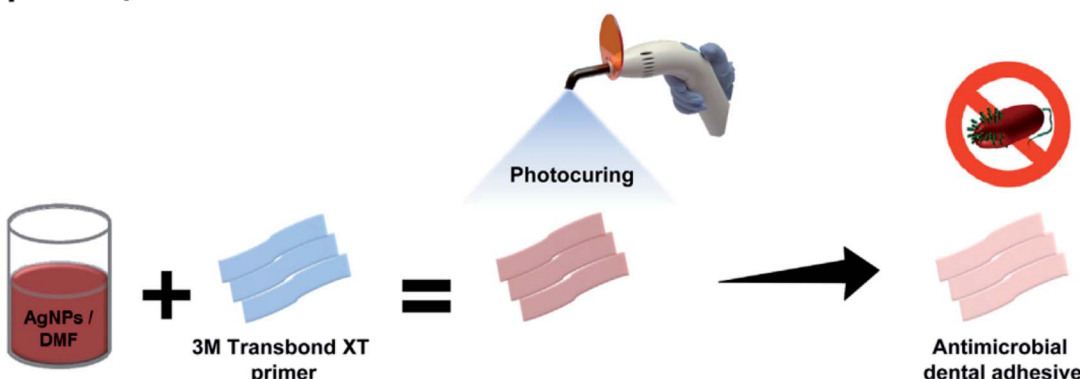


Fig. 8 Schematic illustration of the preparation of Ag NPs and the hybrid dental resin.<sup>149</sup>

to wear and enhance mineralization-induced activities in the case of wearing resin composites; MCS NPs or the resin composites could be applied as multifunctional restorative materials for potential dental applications.<sup>152</sup>

Cevik *et al.* evaluated the influence of hydrophobic nanoparticle silica and pre-polymer on the flexural strength, surface roughness, surface hardness, and resilience of a denture base acrylic resin. Statistical analyses found significant difference between these groups. Each group possessed weak flexural strength in comparison to the controls ( $p < 0.05$ ). In terms of the resilience, silica 5% had the maximum value, while silica 1% possessed the minimum value. For Shore D hardness, silica 1% exhibited the minimum hardness, while addition of the polymer had no significant effects on the acrylic resin's hardness ( $p < 0.05$ ). Silica 1% showed maximum roughness in comparison to the other groups ( $p < 0.05$ ). The incorporation of silica and pre-polymer into the acrylic resin had contrary impacts on the acrylic resin's flexural strength in comparison with the controls. For each concentration, pre-polymer incorporation led to higher flexural strength of the acrylic resins in comparison with silica addition. Higher concentrations of the fillers led to higher mechanical features of the acrylic resin.<sup>153</sup>

Ghahremani *et al.* illustrated that the addition of  $\text{TiO}_2$  NPs to the acrylic resin improved its mechanical features with a reverse impact on its color; the mean tensile strength of the reinforced group was considerably greater (difference of 11 MPa) compared to the controls ( $P = 0.001$ ). The mean effective

strength of the potent group was about 7 MPa greater compared to the controls and the differences were not statistically significant ( $P = 0.001$ ). The color of the modified acrylic resin strengthened with 1 wt%  $\text{TiO}_2$ , which was accompanied by increase in the tensile and impact strength in comparison with the traditional acrylic resin. Hence,  $\text{TiO}_2$  NPs could be added into the acrylic resin powder for a modified color to enhance its tensile and impact strength, if they do not possess any reverse effects on other features.<sup>154</sup>

Sodagar *et al.*'s study evaluated the mechanical and antimicrobial features of composite resins modified by the addition of  $\text{TiO}_2$  NPs. Each concentration of  $\text{TiO}_2$  NPs showed a remarkable impact on the creation and extension of the suppression region including the decline in the colony counts for *S. mutans* and *S. sanguinis*. The composite with 10%  $\text{TiO}_2$  NPs had a considerable impact on the decrease in the colony count for *S. sanguinis* and *S. mutans* (3 days). The controls accounted for the maximum mean shear bond strength, whereas the maximum amount was observed for the 10% NPs composite. The incorporation of  $\text{TiO}_2$  NPs into the composite resins gave anti-bacterial features to the adhesives, whereas the mean shear bond of the composite with 1% and 5% NPs proved to be a reasonable range.<sup>155</sup>

Rodrigues *et al.* characterized the synthesized brushite NP ( $\text{CaHPO}_4 \cdot 2\text{H}_2\text{O}$ ) and demonstrated that functionalization can be regulated based on the concentrations of triethylene glycol dimethacrylate (TEGDMA) employed in the synthesis. Although



the concentration of TEGDMA did not influence the size of the NPs, no reduction in agglomeration was observed. Experimental composites with 10 vol% of the brushite agglomerates and 50 vol% of the silanated glass particles had mechanical features identical to that of a commercial micro-hybrid restorative composite applied in regions exposed to serious occlusal loadings. Therefore, the composite comprising brushite NPs functionalized with higher TEGDMA contents exhibited better performance in the mechanical test in water after 28 days, which had the same fracture strength as that of the commercial controls. The NPs functionalization with TEGDMA had no adverse impact on the ion releases.<sup>156</sup>

Meena *et al.* added various weight percents of nano-alumina (5–20 wt%) and marble dust powder (5–20 wt%) to the base monomer system with bisphenol-A glycidyl methacrylate, camphorquinone, tri-ethylene glycol dimethacrylate, and dimethyl aminoethyl methacrylate in order to fabricate a dental composite. The experimental results showed that the addition of 5 wt% nano-alumina enhanced the hardness and compressive strength by about 88.46% and 23.25%, respectively, while the addition of 5 wt% marble powder augmented the hardness and compressive strength by about 51.27% and 21.2%, respectively. Dynamic mechanical analyses demonstrated that the addition of nano-alumina up to 20 wt% enhanced the storage modulus by about 112.2%, while the addition of marble powder up to 20 wt% augmented the storage modulus by about 191.2%. The conclusion is that regardless of the economic aspects, the marble dust powder-filled dental composite had more acceptable thermo-mechanical and thermal features compared to those of the nano-alumina-filled dental composite.<sup>157</sup>

Al-Ajely *et al.* described calcium fluoride NPs (CaF<sub>2</sub> NPs) applied in dental composites as the dental filling composition of glass type. A coprecipitation technique through binary liquid was employed to prepare the CaF<sub>2</sub> NPs. X-ray diffraction was used to predict the crystal structure characteristics and elemental compositions of the CaF<sub>2</sub> NPs, showing crystalline peaks of the material. EDX analysis was applied for obtaining the elemental composition. Moreover, the SEM images showed the particle size to be  $\sim 58 \pm 21$  nm.<sup>158</sup>

Campos *et al.* studied the experimental dental restorative composites and their development by the addition of montmorillonite (MMT) NPs in a polymer matrix-based BisGMA/TEGDMA for assessing the feasibility of a distinct dimensional behavior during photo-polymerization. The researchers demonstrated that the experimental composites filled with MMT NP have statistically identical polymerization shrinkage values (by thermal mechanical analyses) at the concentration of 30% and less polymerization shrinkage values at the concentration of 50% than the composites that became full with barium glass (BG-control groups).<sup>159</sup>

Al-Mosawi and Al-Badr assessed the efficiency of ZnO NPs, which were incorporated into the composite resin as anti-microbial agents against bacteria that cause dental caries in the oral cavity. The anti-bacterial impacts of inorganic anti-bacterial agents was evaluated through agar disc diffusion test with three different concentrations of the synthesized ZnO NPs (*in vitro*) on the caries-causing bacteria in this research. Finally,

85% decline in the growth of various types of bacteria was revealed. The anti-bacterial agent (ZnO/NPs) had powerful anti-bacterial activities against a broad-spectrum of pathogenic caries-causing bacteria in the oral cavity.<sup>160</sup>

Size-controlled mono-dispersed silica NPs (MSNPs) in the size range from 20 to 330 nm were effectively synthesized through internal circulation rotating packed bed (ICRPB) and blended with freeze-drying in a high-gravity environment (Yang *et al.*). In comparison with the conventional stirred tank reactor, ICRPB decreased the reaction duration by  $\frac{1}{3}$  times and MSNPs with a clearly lower dimensions from 75 nm to 35 nm were obtained. Increasing the MSNPs contents from 40 wt% to 70 wt% enhanced the composite's mechanical features considerably, so that it initially augmented and afterwards declined due to enhancement of the particle size, and reached the highest value at 80 nm. Because of the very good dispersion, the highest MSNPs contents were 30% greater than the commercial silica NPs with a similar size, which provided more acceptable features for the composites.<sup>161</sup>

Bezerra Dias *et al.* made a composite resin that is commercial and contains TiO<sub>2</sub> and Ag covered with TiO<sub>2</sub> NPs for providing anti-bacterial capacities without eliminating the physical and mechanical features. The null hypothesis experimented in this research is that the addition of small amounts of TiO<sub>2</sub> and Ag decorated TiO<sub>2</sub> NPs to a composite resin (a commercial one) had no effect on the compressive and diametric tensile strength, anti-bacterial activities, conversion degree, and surface roughness.<sup>162</sup>

Ai *et al.* suggested a functional nano-fibrous filler and experimented with it to prepare an anti-bacterial composite resin. The aim was to produce hydroxyapatite (HA) nano-wires through the hydrothermal method, dopamine (DA) modification, and loading the silver NPs (Ag NPs). Such Ag NPs laden HA nano-wires were blended into the Bis-GMA/TEGDMA resin for preparing the cured composites. It was assumed that the dispersion of the HA nano-wires and the Ag NPs in the composite resins was homogeneous in terms of the properties of polydopamine (PDA) surface modification. Then, the mechanical features, release of silver ion, cyto-toxicity, and anti-bacterial activities were assessed. The researchers targeted the clinical applications and favorably postulated that the 1D Ag NPs-laden HA nano-wires can be used as effective reinforcements for the composite resin with increased anti-bacterial activities.<sup>163</sup>

Wang *et al.* dealt with the reinforcement and anti-bacterial impacts of cellulose nanocrystal/zinc oxide (CNC/ZnO) nano-hybrids on dental resin composites (DRCs), which was procured *via* precipitation of Zn<sup>2+</sup> on the CNC surface (Fig. 9). In comparison to the DRCs with no CNC/ZnO nano-hybrids, DRCs with 2 wt% CNC/ZnO nano-hybrids had greater compressive strength and flexural modulus, and no significant difference ( $P > 0.05$ ) was observed in the flexural strength and Vickers micro-hardness. The excessive application of the CNC/ZnO nano-hybrids degraded the mechanical features of the DRCs with the exception of the flexural modulus. The DRCs with CNC/ZnO nano-hybrids had very good anti-bacterial features and 78% decrease in the bacterial numbers were achieved with the



addition of 2% CNC/ZnO nano-hybrids. The synthesized DRCs would be useful for addressing bulk fracture and secondary caries.<sup>164</sup>

Wang *et al.* synthesized wrinkle-structured mesoporous silica NPs for inclusion in dental composites wherein the BisGMA/TEGDMA based-resin composites were synthesized *via* silanized silica NPs as the unimodal filler with various loading performances (25, 30, and 35 wt%). In comparison to regular silica particles (Si507), the silica NPs possess center radial wrinkles that are suitable for forming micro-mechanical bonds, which enhanced the filler matrix interfacial interaction and mechanical features. Bimodal silica NPs fillers with either silica NPs-Si90 or silica NPs-Si190 were proposed for producing the resin composites, each of them providing 60 wt% filler loading and eliminating the loading limitations of uni-modal silica NPs (35 wt%). It was found that bimodal silica NPs fillers could significantly augment the mechanical characteristics of the resulting composites. The silica NPs-Si190 filled composite having an optimal mass ratio of 10 : 90 (wt/wt) had the most acceptable mechanical function, which indicated acceptable reinforcing efficacy of the silica NPs and the benefits of the use of bimodal fillers. Silica NPs are potential inorganic fillers to design and fabricate dental resin composites with reasonable mechanical features.<sup>165</sup>

Paiva *et al.* described the use of silver NPs absorbed into a single phase, which was synthesized in a poly-electrolyte

solution, which is the major compound of glass ionomer cement. They carried this out *via* UV irradiation with no changes in the viability of the net setting reaction. It was found that the molar ratio of  $\text{Ag}^+/\text{COO}^-$  and UV exposure duration are significant variables in the procedure. Group D-High Ag specimens generated  $\text{AgNO}_3$  0.5% and TA 10% by mass, for 90 min of UV exposure, which showed considerable difference in inhibiting bacterial development and *Streptococcus mutans* bio-film viability in comparison with the negative controls (group A with no Ag). Nano Ag-glass ionomer cement confirmed the anti-bacterial impacts of diffusion due to oxidative dissolution of silver ions from the cement matrix, which influenced caries arrest and the prevention of developing oral bio-films on their surfaces.<sup>166</sup>

Sundeep *et al.* conducted a study to synthesize clean, eco-friendly, and affordable silver NPs in bulk. The synthesized silver NPs were reinforced with glass ionomer cement for meeting the above two limitations concurrently. Reinforcing Ag NPs in the glass ionomer cement augmented the hardness of traditional glass ionomer cement and accordingly eliminated the limitations of secondary caries caused by bacterial colony surrounding the glass ionomer cement fixed restoration post-medication. A comparison was made between the increase in the hardness of the Ag NP-reinforced glass ionomer cements and traditional glass ionomer cement. Then, the micro-silver reinforced glass ionomer cement and the anti-microbial

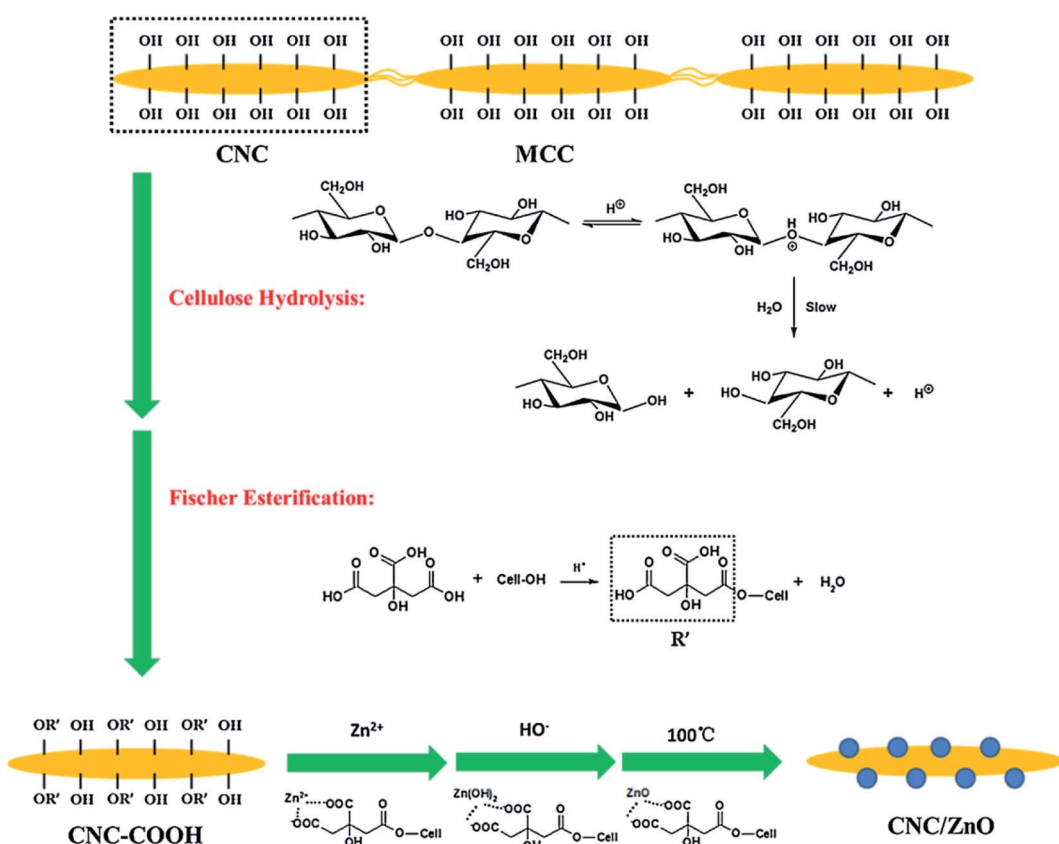


Fig. 9 The preparation route of cellulose nanocrystal/zinc oxide (CNC/ZnO) nanohybrids.<sup>164</sup>



activities of Ag NPs were implemented on *Staphylococcus aureus* and *Escherichia coli* bacteria.<sup>167</sup>

Garcia *et al.* assessed the anti-bacterial activities of zinc oxide NPs absorbed into the self-cured glass ionomer cement and light-cured resin-reinforced GIC on the *Streptococcus mutans* bio-film. GICs, Fuji II (GC America), and Fuji II LC (GC America) were absorbed with NPs at the concentrations of 0%, 1%, and 2% by weight, and the biofilm maturation duration was studied for 1 and 7 days; circular samples of all the GIC types were prepared. The anti-bacterial activities were assessed *via* determination of the number of colony forming units of *Streptococcus mutans* strain in each milliliter. The analyses of glass ionomer cement altered by light-polymerized resin indicated that just the maturing duration had a significant effect on the number of the adhered cells on the bio-film (p50.034, F54.778). If the biofilm is more mature, the number of cells will be greater. SEM analyses did not reveal any changes in the cell morphology associated with the kind of glass ionomer cement, maturation duration, and NP concentrations. The study found that including zinc oxide NPs at the concentrations of 1% and 2% by weight into the glass ionomer cement did not enhance their anti-microbial activities against *Streptococcus mutans*.<sup>168</sup>

Stewart *et al.* presented a newly fabricated broad spectrum anti-microbial drug, mesoporous silica NPs (MSNs), co-assembled for extended releases. Fig. 10 depicts a great payload absorbed into the dental adhesives. The oral degradative environment regulated the release of the templating drugs and octenidine di-hydrochloride, which was mathematically modelled for predicting the efficient service-life. The steady state release killed the cariogenic bacteria without toxicity *via* the prevention of biofilm formation on the adhesive surfaces. The above substance might expand the dental restoration service-life and can be deployed to other durable medical device tissue interfaces for releasing responsive drugs in the case of bacterial infections.<sup>169</sup>

Han *et al.* designed a technique for synthesizing Janus NPs through a selective etching or modification procedure at the Pickering emulsion interface wherein the Janus structure of SiO<sub>2</sub> NPs was confirmed. The amino groups changed one side, whereas the acrylate groups altered the other side. The addition of the Janus NPs as compatibilizers into the adhesives with no cyto-toxicity enhanced the dentin bond strength. The amino groups of the Janus NPs can be attributed to such a situation, which might combine with the carboxyl groups of the imprinted dentin to augment the adhesive penetrability to the dentin (validated by the enhanced resin tags). In addition, the adhesive phase separation might decline. Thus, the Janus NPs can be potential substitute materials for 2-hydroxyethyl methacrylate in dental adhesives.<sup>170</sup>

Azad *et al.* determined the impacts of structural adhesive elements and also dealt with the impacts of incorporating BTDMA, a dimethacrylate monomer-based on BTDA (3,3',4,4'-benzophenone tetracarboxylic dianhydride) with carboxylic acid functions as a functional monomer, and three photoinitiators, butanedione, phenyl-propanedione, and camphorquinone amine on the shrinkage behavior of an experimental dentin bonding system. Additionally, the researchers investigated the impacts of the incorporating silica NPs and BTDMA on mechanical features and adhesion strength of dentin adhesive. Incorporating the silanized silica NPs into adhesive exhibited greater binding strength and mechanical features at very small filler content of 0.2–0.5 wt%.<sup>171</sup>

Liu *et al.* found new orthodontic adhesive, which combined the anti-bacterial activities of 2-methacryloylethyl dodecyl methyl ammonium bromide (MAE-DB) and demineralization preventive feature of amorphous calcium phosphate (NACP) NPs for combating the bio-films and white spot lesions during orthodontic therapy. In comparison with a commercial orthodontic adhesive, the experimentally filled PND adhesive with 5% MAE-DB and 40% NACP showed a higher decline in biofilm development, stopped demineralization, and had no adverse

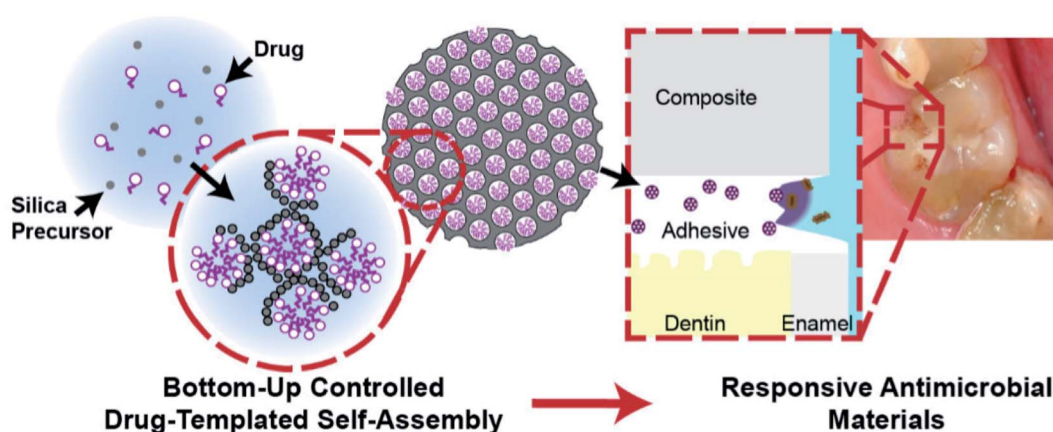


Fig. 10 Bottom-up controlled self-assembly of drug-silica mesoporous nanoparticles enables the long-term release of the antimicrobial agent at the site of recurrent caries: the restoration of the tooth interface. Utilizing a surfactant-like antimicrobial agent, mesoporous silica nanoparticles are inherently maximally loaded with the drug and exhibit extended controlled release. When incorporated into a dental restorative resin adhesive, these mesoporous silica nanoparticles release drug within the restoration-tooth marginal interface, killing caries-causing bacteria, thus extending the service life of the restoration through recurrent caries prevention.<sup>169</sup>



effect on the shear bond strength. If the anti-bacterial impacts of MAE-DB combined with the remineralization approach of NACP, it can be followed by opportunities of applications in nano-technology materials for reducing the burden of dental caries throughout the world.<sup>172</sup>

Yue *et al.* designed a self-healing adhesive containing anti-microbial and remineralizing abilities, and explored the unprecedented impacts of incorporation of micro-capsules, dimethyl-aminoxyhexadecyl methacrylate (DMAHDM), and NPs of amorphous calcium phosphate (NACP). Poly(urea-formaldehyde) (PUF) shells with triethylene glycol dimethacrylate (TEGDMA) as a therapeutic liquid were used to synthesize self-healing micro-capsules; the new adhesive included 10% DMAHDM, 7.5% micro-capsules, and 20% NACP. A single edge V-notched beam technique was employed for measuring the fracture toughness  $K_{IC}$  and the autonomous crack-healing efficacy with experiments on an oral plaque microcosm bio-film model. This newly constructed self-healing, anti-microbial, and remineralizing dental adhesive corresponded to the dentin bond strength of a commercial control ( $p > 0.1$ ); it attained substantial crack healing with very good  $K_{IC}$  recovery of 67%. It possessed powerful anti-microbial activities, decreased the bio-film colony forming units by about 4 orders of magnitude, and decreased the bio-film acid generation to 1/100th of that of the bio-films on the commercial control resin.<sup>173</sup>

Al-Qarni *et al.* conducted a study for developing a calcium (Ca) and phosphate (P) ion-rechargeable and protein repellent adhesive with NPs of amorphous calcium phosphate (NACP) and 2-methacryloyloxyethyl phosphorylcholine (MPC); the impacts of MPC on the ion re-charge and re-release was examined. It was found that the addition of NACP + MPC did not demonstrate any negative effects on the dentin binding strength ( $p > 0.1$ ). As the number of re-charge/re-release cycles increased, the Ca/P ion re-release achieved accordingly greater levels ( $p > 0.1$ ), which indicated enduring re-mineralization abilities; one re-charge made it possible for the adhesives to continue re-releases for 21 days. The incorporation of 3% MPC was followed by a 10-fold decline in the protein absorption and 1-2 log decline in the bio-film CFU. The re-chargeable adhesive containing MPC + 30% NACP significantly decreased protein absorption, bio-film development, and lactic acid. The incorporation of MPC did not endanger the very good Ca/P ion release, re-chargeability, and dentin bond strength. This adhesive has the potential for various tooth restoration applications for inhibiting caries and increasing the restoration durability.<sup>174</sup>

Xie *et al.* designed an adhesive with the three advantages of recharging calcium phosphate ion, protein repellent, and anti-bacterial function. MPC and dimethyl-aminoxyhexadecyl methacrylate (DMAHDM) were assimilated into a NACP rechargeable adhesive for achieving protein repellent and anti-bacterial abilities for combating bio-films and caries. The new bio-active adhesive exhibited powerful protein repellent ability and considerably decreased the bacterial binding and viabilities by declining the bio-film colony shaping units by nearly 4 log in comparison with the commercial control. The bio-active adhesive containing dental plaque microcosm bio-film culture retained a pH > 6, whereas the commercial control adhesive

possessed a cariogenic pH = 4. The adhesive with these three advantages has the potential for protecting tooth structures and inhibiting biofilms and caries formation. The combination procedure for NACP, MPC, and DMAHDM with three benefits will hopefully find application in a variety of dental restorative and preventive substances for reducing plaque formation and inhibiting caries.<sup>175</sup>

Liang *et al.* examined poly(amido amine) (PAMAM), NPs of amorphous calcium phosphate (NACP) adhesive, and PAMAM + NACP adhesive to remineralize dentin in lactic acid with no initial P and Ca ions. Maximum dentin remineralization in this highly challenging environment was used to obtain new PAMAM + NACP. It made the composite-dentin bond longer and suppressed caries in patients with dry mouths, in which local pH is frequently acidic and there is a lack of saliva with P and Ca ions. PAMAM could not generate remineralization in lactic acid. Using NACP adhesive, P and Ca ions' release was observed, which increased the pH to 6.5, and attained minor remineralization in such a challenging environment. PAMAM + NACP was synergized and NACP presented necessary Ca and P ions, enhanced pH, and enabled PAMAM for fulfilling its nucleation template functions. It was followed by maximum remineralization and restoration of the hardness of the demineralized dentin to the hardness of the healthy dentin. PAMAM + NACP has potential for patients with lower saliva and radiation caries and for a variety of dental restorations for prolonging the bonded interface, inhibiting secondary caries, remineralization, and protecting the tooth structures.<sup>176</sup>

Dutra-Correa *et al.* assessed the impacts of small Ag NPs absorption concentration (50 ppm increment from 50 to 250 ppm) into the primer of a 3-step, which is found in the market as an etch-and-rinse adhesive system. NPs functionalized with appropriate organic stabilizers controlling the particle size and reducing agglomeration were substantially prepared and poured into the primer, which generated hydrophilic and functional materials even at small Ag NP concentrations.

The lowest suppressive concentrations were observed between 25 and 50 ppm Ag NPs, the lowest being at 50 ppm of Ag NPs. The suppression of bacterial activities was greater with respect to the controls in each Ag NP group in comparison with the controls in the agar diffusion assay; biofilm suppression was greater in 250 ppm Ag NPs as compared to the controls. Each Ag NP group and Scotch bond Multi-Purpose adhesive system showed the same cyto-toxicity in all periods. The adhesives bearing 200 and 250 ppm Ag NPs and Scotch bond Multi-Purpose adhesive system (controls) had maximum Microtensile Bond Test values, which are identical to the ones in Scotch bond Multi-Purpose adhesive system control in both the cases (24 h and 6 months) ( $p > 0.05$ ). Ag NPs/primer relationship may defend the tooth adhesive interface, which increases the dental restoration durability.<sup>177</sup>

Polymethyl methacrylate (PMMA) thin films absorbed with bio-fabricated silver NPs have been not employed for evaluating the *in vitro* anti-microbial and anti-biofilm activities against cariogenic bacterium *Streptococcus mutans* (Thomas *et al.*). *Bacillus amyloliquefaciens* SJ14 culture (Mag NPs) and extract from *Curcuma aromatica* rhizome (Cag NPs) were used to



generate silver NPs. Moreover, the lowest suppressive concentrations, lowest bactericidal concentrations, and anti-biofilm activities of Ag NPs against *Streptococcus mutans* were evaluated wherein Mag NPs displayed better anti-microbial activities in comparison to Cag NPs. Furthermore, the Mag NPs and Cag NPs exhibited 99% and 94% suppression of biofilm formation of *Streptococcus mutans* at concentrations of  $3 \mu\text{g mL}^{-1}$  and  $50 \mu\text{g mL}^{-1}$ , respectively. The Ag NPs were additionally absorbed into the PMMA thin films through solvent casting technique. PMMA/Mag NPs and PMMA/Cag NPs nano-composite thin films were exposed to anti-microbial and anti-biofilm analyses. In addition, microbicidal activities were greater for the PMMA/Mag NPs thin film, showing the potential of microbially synthesized Ag NPs as agents for inhibiting cariogenic bacteria from colonizing the dental restorative materials.<sup>178</sup>

A polymeric composition comprises modified-TiO<sub>2</sub> nanoparticles, with or without a solvent, and polymer precursors, wherein the modified-TiO<sub>2</sub> nanoparticles comprise titanium dioxide nanoparticles, which are modified with a short-chain unsaturated compound that comprises 2 to 10 carbon atoms. The polymeric composition can be used in dental compositions such as dental adhesives, dental composites, and dental sealants.<sup>179</sup>

Balasankar *et al.* provided a treatment approach for delivering chlorhexidine (CHX) loaded poly(lactic-*co*-glycolic acid) (PLGA) NPs *via* dentinal tubules of demineralized dentin substrates for probable applications in adhesive and restorative dentistry. The formulated CHX loaded PLGA NPs had interesting physico-chemical features, negligible cyto-toxicity, potential anti-bacterial efficiency, and slow degradation patterns related to the capability of releasing CHX for up to 28 days. CHX loaded PLGA NPs in aqueous solution can penetrate and infiltrate *via* dentinal tubules up to 10  $\mu\text{m}$  depth, which have a close association with the resin tags after binding resin infiltration.<sup>180</sup>

Gutiérrez *et al.* assessed the impact of adding copper NPs (Cu NPs) at various concentrations into a two-step etch-and-rinse (2 ER) adhesive on the anti-microbial activities (AMA), copper release (CR), degree of conversion (DC), water sorption (WS), solubility (SO), immediate (IM), ultimate tensile strength (UTS), 1 year resin dentin bond strength ( $\mu\text{TBS}$ ), and nano-leakage (NL). The addition of Cu NPs presented AMA towards the adhesives at each concentration. Greater CR was seen in adhesives with greater concentrations of Cu NPs. DC, UTS, SO, and WS was not affected. An increase was seen for  $\mu\text{TBS}$  in the 0.1 and 0.5% copper groups. A considerable decline was found for NL in each group as compared to the controls. After 1 year, any remarkable reductions in  $\mu\text{TBS}$  and any considerable increase in NL were not found for copper with adhesives in comparison with the controls. The addition of Cu NPs at concentrations up to 1 wt% in the 2 ER adhesive can be an option for providing AMA and preserving the bond to dentin with no reduction in the adhesive's mechanical features.<sup>181</sup>

The same group examined 2 year (2Y) resin dentin  $\mu\text{TBS}$  and NL. The addition of copper NPs up to 0.5 wt% exhibited anti-microbial features towards ER adhesives and stopped the

degradation of the adhesive interface with no reduction in the mechanical features of the formulations.<sup>182</sup>

Georgy *et al.* examined the dental adhesive composition containing NPs of metals for gaining lengthy bactericidal features by addition of Ag, V, Cu, Fe, Al, and Ta NPs in the dental adhesive, which resulted in its prolonged bacteriostatic and bactericidal impacts *versus* dental plaque microflora. For tantalum NPs, the modifications in the concentrations resulting from the deviation in the working mode of the electric discharge dispersion condensing instrument had no effects on the anti-septic features of the resulting product of the dental adhesive. It was observed that tantalum NPs enhance the average value of shear strength in the system filling the material adhesive dentin up to over 40%. With regards to the bactericidal and high adhesion features, tantalum NPs as an additive for dental adhesive have advantages that need to be exploited.<sup>183</sup>

Rizk *et al.* demonstrated identical bioactive potentials of poly-hedral oligomeric silsesquioxanes (POSS) particles as that of nanosized bio-active glass (BG-Bi) particles when they were blended with the adhesive while maintaining suitable mechanical features of the system. The impacts of the multi-functional POSS NPs on the degrees of conversion, sol fraction, and water sorption indicated higher crosslink density of the filled adhesive while maintaining low viscosities. Hence, multi-functional POSS is an attractive option for testing in bond strength tests as it could enhance the binding strength due to the higher cross-linking capability and stop binding strength degradation over time because of its mineralization capacities. Though mono-functional POSS particles resulted in a highly declined conversion and bio-active glass particles strongly enhanced the viscosity, apparently, their application in dental adhesives is limited to specific uses and substances.<sup>184</sup>

Tooth whitening agents were necessarily nano-modified to increase the whitening efficiency and decrease their harmful side effects. For example, calcium peroxide nanoparticles could penetrate deeper into the tooth structure through micro and nano cracks, make longer surface contact, and increase the effectiveness of the whitening agent.<sup>185</sup>

## 6.5. Nano-materials for periodontics

Periodontitis is a dental inflammatory dysfunction, which influences the surrounding structures of the teeth (periodontium). This disease is described by inflammation and decay of the surrounding teeth and supporting tissues, namely, periodontal ligament, alveolar bone, cementum, and gum, which are commonly encountered due to anaerobic Gram-negative bacterial invasion of the teeth.<sup>186,187</sup> New advancements in nano-materials and nano-technology has offered hopeful chances and opportunities for the efficient management of periodontitis. A number of the most acceptable findings and benefits can be attained from such newer strategies that include the application of bio-adhesive polymers for achieving lengthy drug release, increase in intrapocket drug penetration, increase of mechanical features *via* chemical cross-linkers, and possible



loading of multiple drugs in a unit delivery system. The above rewards could provide the ground for further research opportunity in developing drug delivery systems, which will advance dental therapeutics.<sup>188–191</sup>

Khan *et al.* performed a study to synthesize bio-active electro-spun fibers for bio-medical and dental application with higher biocompatibility. The *in situ* precipitation of nanohydroxyapatite (nHA) was administered at different concentrations (0.5%, 1%, 2%, 3%, and 5% wt/wt) of the functionalized multiwalled carbon nano-tubes (MWCNTs) through microwave (MW) irradiation method. HA/CNT and CNT were silanized with  $\gamma$ -methacryloxypropyl-trimethoxysilane (MPTS), blended with poly-vinyl alcohol (10% wt/vol), and electrospun for fabricating the fibers. The bio-compatibility of the two fibers was accessed due to their impacts on angiogenesis in chick chorioallantoic membrane (CAM) assay. The mechanical features indicated greater compressive strength of the 3% loaded HA/CNT ( $100.5 \pm 5.9$  MPa) in comparison with the other features and failure behavior represented the dispersion of CNT in the HA matrix. The HA/CNT electrospun fibers demonstrated higher blood vessel formation in comparison with the CNT fibers. Such HA/CNT electrospun fibers revealed advantageous objectives in terms of the biocompatibility. Of course, due to the greater mechanical features of CNT reinforced composites, they may be employed for the regeneration of pulp-dentin and periodontal (Fig. 7).<sup>192</sup>

Khajuria *et al.* designed a chitosan-based risedronate or zinc-hydroxyapatite intra-pocket dental film (CRZHDF) for use in treating alveolar bone loss in the rat model of periodontitis. Periodontitis was generated through *Porphyromonas gingivalis*-lipopolysaccharide injection surrounding the mandibular first molar and the rats were classified into five groups (12 rats per group): periodontitis plus chitosan film, periodontitis plus CRZHDF-B, healthy, untreated periodontitis, and periodontitis plus CRZHDF-A. After 4 weeks, blood samples and mandibles were taken for bio-chemical, radiographic, and histological analyses. Bone specific alkaline phosphatase activities and tartrate resistant acid phosphatase 5b were less in CRZHDF-A and CRZHDF-B groups in comparison with the untreated periodontitis group ( $p < 0.0001$ ); osteocalcin expression was greater in the CRZHDF-A and CRZHDF-B groups in comparison with the un-treated periodontitis group ( $p < 0.0001$ ). Alveolar bone was intact in the healthy group. A local injection of CRZHDF led to remarkable improvement in the mesial and distal periodontal bone support (MPBS & DPBS) proportions (%), bone mineral density, and inverse alveolar bone resorption as compared with the un-treated periodontitis group ( $p < 0.001$ ). This study revealed that new CRZHDF therapy efficiently declined alveolar bone demolition and contributed to periodontal treatment in the rat model of experimental periodontitis.<sup>193</sup>

Mahapatra *et al.* synthesized cerium oxide nano-materials (Ce NMs) with various directional forms (aspect ratios) by a pH managed hydrothermal procedure and treated them with stem cells extracted from human dental pulp at different dosages. Small Ce NMs (NPs & nano-rods) were internalized quickly by the cells, whereas long Ce NMs (nano-wires) were gradually internalized, which resulted in various distributions

of Ce NMs and inhibited the ROS levels intra-cellularly or extra-cellularly under  $H_2O_2$ -exposed condition. When the stem cells were given a dose with Ce MNs, they were found to possess very good cell survivability and damage from intra-cellular elements such as DNA fragmentation, lipid rupture, and protein degradation was considerably dropped. Therefore, ROS scavenging episodes of Ce NMs require specific attention for aspect ratio dependent cellular internalization. Moreover, these findings indicated the potential application of Ce NMs for protecting stem cells from ROS environments that may eventually enhance stem cell potentials for tissue engineering and regenerative medicine applications.<sup>194</sup>

Xia *et al.* developed iron oxide NPs, which incorporated calcium phosphate cement scaffolds (IONP-CPC) and achieved considerable improvements in osteogenic differentiation of human dental pulp stem cells (hDPSCs) into IONP-CPC scaffolds. CPC features such as more satisfactory wetting, higher protein absorption, and higher cell binding and spreading were ameliorated by addition of IONPs. Osteogenic differentiations of hDPSCs were considerably increased by incorporating IONP into CPC. A considerable improvement was attained in ALP activities and expression of the osteogenic gene. The bone matrix mineral, which was synthesized by the cells, was enhanced two-to three-folds in comparison with the mineral with no IONPs. Higher cell function was ascribed to the IONP-CPC scaffold nanotopography and IONPs releases and intakes within the hDPSCs. Remarkable improvements were noted in osteogenesis, indicating that the newly developed IONP-CPC scaffolds would be potentially useful for bone tissue engineering and re-generative medicine applications.<sup>195</sup>

Ji *et al.* specified a technique, which could efficiently deliver treatment agents to the pulp and was based on using NPs that could actively be directed by magnetic forces to the pulp and travel across natural channels in dentin (middle layer of the teeth). The technique could reduce inflammation of the damaged pulp and enhance the penetration of dental adhesives into the dentin. The above delivery approach is affordable with lower pain and lower traumatic events compared to the current treatment choices for the treatment of the damaged dental pulp. It is straightforward and its translation to clinical applications can be accomplished easily (Fig. 11).<sup>196</sup>

Xia *et al.* made a calcium phosphate cement with gold NPs (GNP-CPC) and examined its osteogenic induction capability on hDPSCs. The incorporation of GNPs enhanced the hDPSCs behavior on CPC such as more acceptable cell adhesion (about two-fold enhancement in cell spreading) and rapid growth, and enhanced osteogenic differentiation ( $\sim 2\text{--}3$ -fold increase in 14 days). GNPs provided CPC with a nanostructure, which improved the surface features for cell adhesion and the following behaviors. GNPs released from GNP-CPC were internalized *via* hDPSCs, which was confirmed by transmission electron microscopy (TEM) and enhanced cell performance. Culture media with GNPs increased the cellular activity of hDPSCs. This had consistency with GNP-CPC outputs and confirmed osteogenic induction. Finally, GNP-CPC remarkably augmented the osteogenic performance of hDPSCs, thus



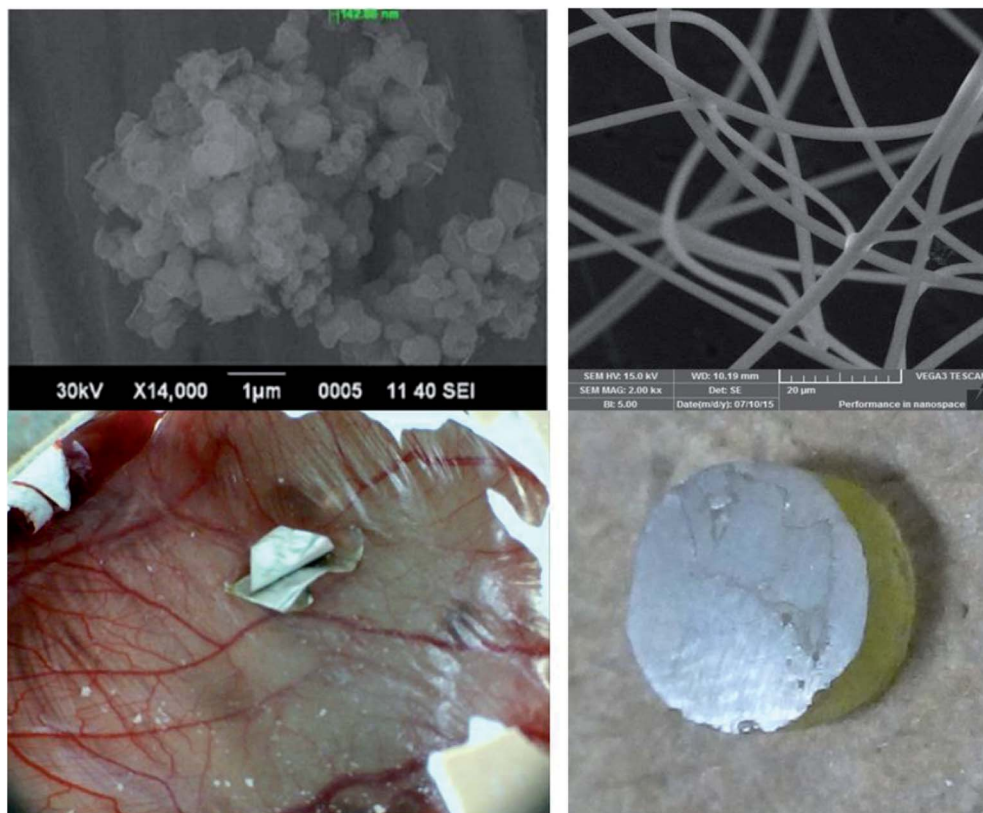


Fig. 11 Fabrication and *in vivo* evaluation of the hydroxyapatite/carbon nanotube electrospun fibers for biomedical/dental applications.<sup>192</sup>

rendering GNPs as a good candidate for modifying CPC with nano-topography, which serve as bio-active additives for increasing bone regeneration.<sup>197</sup>

Anton *et al.* examined the impact of nano-crystalline cerium oxide doped with gadolinium ( $\text{Ce}_{1-x}\text{Gd}_x\text{O}_y$ ) on the morpho-functional features and proliferative activities of mesenchymal

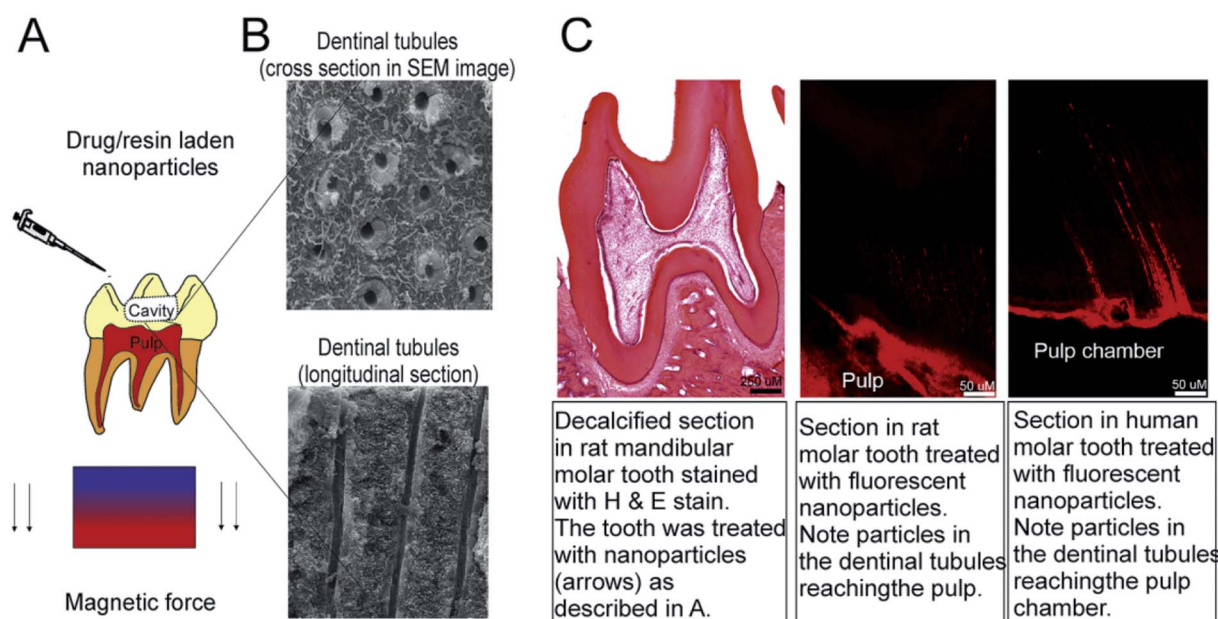


Fig. 12 Technology for steering and delivering the drug-laden nanoparticles to the tooth pulp is described. This technology exploits naturally occurring dentinal tubules that extend from the dentin to the pulp and magnetic forces to actively steer the iron nanoparticles deep into the tooth structure. This technology was tested on rat molar teeth and in freshly extracted human teeth, and can be used to deliver drug-laden nanoparticles to the pulp or to enhance the bond strength of commercially available resin adhesives to the tooth dentin.<sup>196</sup>

stem cells (MSCs) extracted from the dental pulp. They showed that the introduction of  $\text{Ce}_{1-x}\text{Gd}_x\text{O}_y$  NPs into the culture of dental MSCs activated the rapid growth of cells in a dosage-dependent manner. The increased concentration of  $\text{Ce}_{1-x}\text{Gd}_x\text{O}_y$  NPs suppressed the cells' rapid growth but this condition did not result in additional expansion of apoptosis and cell mortality. Anton *et al.* found that nano-crystalline cerium oxide may be viewed as a foundation for developing largely effective and affordable complements to culture MSCs.<sup>198</sup>

Huang *et al.* conducted a study on fabricated mesoporous calcium silicate (MesoCS) NPs with osteogenic, drug delivery, and anti-bacterial features for endodontic materials, which has a very good capability for developing apatite mineralization. They found that 200 nm sized MesoCS NPs synthesized *via* a simple template technique had a higher specific surface area and pore volume with internal mesopores (average pore size = 3.05 nm). MesoCS NPs might be employed as drug carriers for maintaining long-term release of gentamicin and fibroblast growth factor-2 (FGF-2). MesoCS-loaded FGF-2 could trigger more odontogenic proteins compared to CS due to FGF-2 release. MesoCS NPs are potentially beneficial endodontic materials as bio-compatible and osteogenic dental pulp tissue regenerative materials (Fig. 12).<sup>199</sup>

Table 1 lists the applications of nano-materials in dentistry. It shows the developments and individual procedures, which have been formerly discussed.

## 7. Toxicity of nano-materials

Although it is expected that nano-materials can have a great impact on a large range of industrial and economic sectors, the sustainability of green nano-solutions is not clear yet and it should be carefully treated. In fact, the incorporation of nano-materials can be environmentally friendly, healthy, and safe as well as strongly compete with traditional technologies.<sup>200-208</sup> Nano-materials covertly get introduced into the environment *via* soil, water, and air during different human activities including environmental treatments that intentionally deposit engineered nano-materials into the soil or aquatic systems.<sup>209-216</sup> Magnetic nano-materials enjoy additional benefits, besides smaller sizes and higher reactivity and capacities; thus, they are potential lethal agents as they can induce toxic and harmful cellular impacts, which are not common in the bulkier micron-sized counterparts. Moreover, research has showed that nano-materials can enter organisms *via* ingestion or inhalation and can translocate into different organs and tissues, thus exhibiting hazardous impacts. Even though a number of investigations have dealt with the toxic impacts of nano-materials on plant cells and animal cells, toxicological examinations of magnetic nano-materials on plants have been not performed adequately. The use of Ag nano-materials in several consumer products has resulted in their release in the aquatic environment such that they have become the origin of dissolved Ag with adverse impacts on aquatic organisms such as algae, bacteria, daphnia, and fish.<sup>217-219</sup> Respiratory systems are the main target for the possible toxicity of nano-materials, which is caused by the addition of the inhaled particles to the

portal entries. In addition, it accepts the whole cardiac outputs. Nano-materials have widespread application in biosystems; however, in spite of the fast development and initial acceptance of nano-biotechnology, their potential impacts on the health due to the long-term exposure to different concentrations in human have still not been confirmed. Nonetheless, the study of the environmental impacts of nano-materials will be under extreme scrutiny in the future. Nano-material toxicity is its capability of organizing around the protein molecules, which are dependent on the sizes of the particle, curvature, shapes, surface characteristics, functionalized groups, charge, and free energy. As a result of such binding, a number of nanoparticles have destructive biological outcomes such as protein unfolding, thiol cross-linking, fibrillation, and loss of enzymatic activities. One of the other paradigms is the release of poisonous ions when the thermo-dynamic features of the materials support the dissolving particles in a biological environment or a suspension medium.<sup>220-225</sup> Nano-materials usually accumulate in seawater and hard water and they are highly affected by organic materials or other natural particles (colloids) in fresh water. The dispersion mode can also modify the eco-toxicity; however, several abiotic agents influencing this are salinity, pH, and the existence of organic matters, which should be carefully analyzed using eco-toxicological examinations.<sup>226-228</sup>

## 8. Conclusion and future perspectives

Nano-medicine should resolve challenges in its use, increase understanding of pathophysiological basis of diseases, provide greater diagnostic chances and opportunities, and offer more efficient treatments and preventive features. The purpose of nanotechnology is to exploit the attractive physico-chemical properties of nano-materials in a number of innovative applications that are energy saving as well as economically and environmentally useful, which are expected to impact several economic sectors. These solutions may offer a chance to decrease the pressure of trading renewable energy, to improve the reliability and safety of power delivery systems, as well as to use unconventional water sources or nano-enabled construction products for providing better ecosystem and livelihood conditions. However, the opportunities offered by nano-materials in economic solutions should be balanced by a number of practical challenges, critical environmental and social issues, as well as with human health and safety concerns. In particular, nano-materials may have significant hazardous properties that are still unknown, which are related to their unique physico-chemical properties that can cause risks for a wide range of employees exposed through the overall lifecycle of the nano-materials. Therefore, scientific research, technological, governmental, and workforce efforts should define the hazardous effect of nano-materials to assess the risks adequately. This would provide helpful information in preparing protective measures for comprehensive risk management for both the general and occupationally exposed populations.



Table 1 Selected applications of nano-materials in dentistry

Nano-materials	Shape	Application in dentistry	Ref.
Ag	Nanoparticles	Tooth disinfectant	99
TMP	Nanoparticles	Toothpastes	100
Ag <sub>2</sub> O	Nanoparticles	Toothpastes	101
Ag	Nanoparticles	Toothbrushes	102
NACP	Nanoparticles	Dental sealants	103
Cs	Nanoparticles	Dental varnishes	104
Cs	Nanoparticles	Dental care	105
ZrO <sub>2</sub>	Nanoparticles	Dental care	106
CMC/ACP	Nanoparticles	Dental care	107
Ferumoxytol	Nanoparticles	Biofilms for preventing tooth decay	108
CS-CMS-MMT	Nanoparticles	Biofilms for preventing tooth decay	109
NACP	Nanoparticles	Biofilms for preventing tooth decay	110
pMSN	Nanoparticles	Biofilms for preventing tooth decay	111
Cr	Nanoparticles	Biofilms for preventing tooth decay	112
CuCh NP	Nanoparticles	Biofilms for preventing tooth decay	113
Ag	Nanoparticles	Biofilms for preventing tooth decay	114
nDCPD	Nanoparticles	Biofilms for preventing tooth decay	115
TiO <sub>2</sub>	Nanoparticles	Dental prosthesis	119
TiO <sub>2</sub>	Nanotubes	Dental prosthesis	120
ZrO <sub>2</sub>	Nanoparticles	Dental prosthesis	121
Ag <sub>2</sub> O-TiO <sub>2</sub>	Nanotubes	Implant materials	122
TiO <sub>2</sub> -Ag	Nanotubes	Dental implant	123
Ag-Fe <sub>3</sub> O <sub>4</sub>	Nanoparticles	Dental implant	124
Pd-Ag-HAp	Nanoparticles	Dental implant	125
Cu-TiO <sub>2</sub>	Nanotubes	Dental implant	126
TiO <sub>2</sub>	Nanoparticles	Dental implant	127
Ag	Nanorods	Dental implant	128
Ag	Nanoparticles	Dental implant	129
Ag	Nanoparticles	Dental implant	130
ZnO	Nanorods	Dental implant	131
Au	Nanoparticles	Dental implant	132
NACP	Nanoparticles	Root dentin	138
Ag	Nanoparticles	Root dentin	139
IO	Nanoparticles	Endodontic disinfection	140
Ag	Nanoparticles	Dental resin	149
Ag/QND	Nanohybrids	Dental resin	150
AgBr/BHPVP	Nanoparticles	Dental resin	151
MCS	Nanoparticles	Dental resin	152
SiO <sub>2</sub>	Nanoparticles	Dental resin	153
TiO <sub>2</sub>	Nanoparticles	Dental resin	154
TiO <sub>2</sub>	Nanoparticles	Dental composites	155
CaHPO <sub>4</sub> ·2H <sub>2</sub> O	Nanoparticles	Dental composites	156
Nanoalumina	Nanoparticles	Dental composites	157
CaF <sub>2</sub>	Nanoparticles	Dental composites	158
MMT	Nanoparticles	Dental composites	159
ZnO	Nanoparticles	Dental composites	160
MS	Nanoparticles	Dental composite resin	161
TiO <sub>2</sub> /Ag	Nanoparticles	Dental composite resin	162
HA-PDA-Ag	Nanowires	Dental composite resin	163
CNC/ZnO	Nanohybrids	Dental composite resin	164
SiO <sub>2</sub>	Nanoparticles	Dental composite resin	165
Ag	Nanoparticles	Glass ionomer cement	166
Ag	Nanoparticles	Glass ionomer cement	167
ZnO	Nanoparticles	Glass ionomer cement	168
MSNs	Nanoparticles	Dental adhesive	169
SiO <sub>2</sub>	Nanoparticles	Dental adhesive	170
SiO <sub>2</sub>	Nanoparticles	Dental adhesive	171
NACP	Nanoparticles	Dental adhesive	172
NACP	Nanoparticles	Dental adhesive	173
NACP	Nanoparticles	Dental adhesive	174
NACP	Nanoparticles	Dental adhesive	175
NACP	Nanoparticles	Dental adhesive	176
Ag	Nanoparticles	Dental adhesive	177



Table 1 (Contd.)

Nano-materials	Shape	Application in dentistry	Ref.
Ag	Nanoparticles	Dental adhesive	178
TiO <sub>2</sub>	Nanoparticles	Dental adhesive	179
PLGA	Nanoparticles	Dental adhesive	180
Cu	Nanoparticles	Dental adhesive	181
Cu	Nanoparticles	Dental adhesive	182
Ag, Ta, Cu, Fe, Al and V	Nanoparticles	Dental adhesive	183
BG-Bi	Nanoparticles	Dental adhesive	184
CaO <sub>2</sub>	Nanoparticles	Tooth whitening	185
HA/CNT	Nanofiber	Pulp-dentin and periodontal	192
HA/Zn	Nanoparticles	Periodontitis	193
Ce	Nanowires, nanoparticles, and nanorods	Pulp-dentin	194
IO	Nanoparticles	Pulp-dentin	195
IO	Nanoparticles	Pulp-dentin	196
GNP-CPC	Nanoparticles	Pulp-dentin	197
Ce <sub>1-x</sub> Gd <sub>x</sub> O <sub>y</sub>	Nanoparticles	Pulp-dentin	198
MesoCS	Nanoparticles	Pulp-dentin	199

Generally, nanotechnology should not only provide solutions but should also “become green” with respect to safety and health. In this context, a discussion between experts should be pursued to carefully balance the benefits of green nanotechnology and the potential costs for the society, especially in terms of environmental, public, and occupational health. This consideration will maximize the environmental and societal benefits, health gains, and cost savings.

Recent developments in nano-materials and nanotechnology can provide helpful insights into the commercial applications of nano-materials for the ‘true’ regeneration of periodontal apparatus as a whole, including dentine, cementum, periodontal ligaments, and bone. Scaffolds impregnated with nanoparticles along with tissue engineering triads can mimic an extracellular matrix that can initiate the formation of the host tissues. Thus, given their low toxicity, antimicrobial properties, and enhanced protein–surface interactions, these nanoparticles can be used for various dental applications. Their potential role in the formation of improved biomaterials in different forms is a significant innovation in dentistry. The combination of continual refinements in conventional treatment modalities and advances in the clinical applications of nanotechnology are promising for improving dental care.

## Abbreviations

2 ER	Two-step etch-and-rinse
AgNO <sub>3</sub>	Silver nitrate
ALN	Alendronate
ACP	Amorphous calcium phosphate
Ag NPs	Silver nanoparticles
AMA	Adhesive on antimicrobial activity
Bis-GMA	Bisphenol A-glycidylmethacrylate
BMC	Bioactive multifunctional composite
BET	Brunauer emmett teller
BG-Bi	Bioactive glass
Ca	Calcium
Cag	Curcuma aromatica rhizome
CNC/ZnO	Cellulose nanocrystal/zinc oxide
CMS	Carboxymethyl starch
CHX	Chlorhexidine
CS	Chitosan
CMC	Carboxymethyl chitosan
CR	Copper release
CVD	Chemical vapour deposition
DMAHDM	Dimethylaminohexadecyl methacrylate
DRCs	Dental resin composites
DLS	Dynamic light scattering
EBPADMA	Ethoxylated bisphenol A dimethacrylate
EDX	Energy dispersive X-ray
IR	Infrared
POM	Polarized optical microscopy
LSPR	Localized surface plasmon resonance
ICRPB	Internal circulation rotating packed bed
SDR	Spinning disc reactor
TEGDMA	Triethylene glycol dimethacrylate
UDMA	Urethane dimethacrylate
HA	Hydroxyapatite
DA	Dopamine
PDA	Poly dopamine
PMMA	Poly methylmethacrylate
TMP	Trimetaphosphate
Y-TZP	Yttria-stabilized tetragonal zirconia polycrystals
PO <sub>4</sub>	Phosphate
DMAHDM	Dimethylaminohexadecyl methacrylate
DMAHDM	Dimethylaminohexadecyl methacrylate
MMT	Montmorillonite
PUF	Poly (urea-formaldehyde)
TEGDMA	Triethylene glycol dimethacrylate
H <sub>2</sub> O <sub>2</sub>	Hydrogen peroxide
MAE-DB	2-Methacryloylethyl dodecyl methyl ammonium bromide



MPC	2-Methacryloyloxyethyl phosphorylcholine
MMT	Montmorillonite
NaBH <sub>4</sub>	Sodium borohydrate
NaF	Sodium fluoride
PMMA	Polymethyl methacrylate
ROS	Reactive oxygen species
PLGA	Poly-(lactic-co-glycolic acid)
PMGDM	Pyromellitic glycerol dimethacrylate
CHX	Chlorhexidine
GIC	Glass ionomer cement
hDPSCs	Human dental pulp stem cells
UTS	Ultimate tensile strength
DC	Degree of conversion
WS	Water sorption
SO	Solubility
IM	Immediate
μTBS	1 year resin dentin bond strength
FBPRE	<i>Ficus benghalensis</i> prop root extract
NaClO	Sodium hypochlorite
NL	Nanoleakage
POSS	Polyhedraloligomeric silsesquioxanes
RBC	Resin-based composites
TiO <sub>2</sub>	NPs Titanium dioxide nanoparticles
NACP	Nanoparticles of amorphous calcium phosphate
CS-NPs	Chitosan nanoparticles
IO-NPs	Iron oxide nanoparticles
pMSN	Pore mesoporous silica nanoparticles
MSNPs	Monodisperse silica nanoparticles
CaF <sub>2</sub> NPs	Calcium fluoride nanoparticle
Cu NPs	Copper nanoparticles
nano-ZrO <sub>2</sub>	Zirconium oxide nanoparticles
nDCPD	Dicalcium phosphate dihydrate nanoparticle
SEM	Scanning electron microscope
TEM	Transmission electron microscopy
XRD	X-ray diffraction
XPS	X-ray photoelectron spectroscopy

## Conflicts of interest

There are no conflicts to declare.

## Acknowledgements

This work was financially supported by the Bilingual Teaching Programme of Hainan University (hndsyk 201909); The Key project of the National Social Science Foundation of the year 2018 (18AJY013); The 2017 National Social Science Foundation project (17CJY072); The 2018 planning project of philosophy and social science of Zhejiang province (18NDJC086YB); The 2018 Fujian Social Science Planning Project (FJ2018B067); The Planning Fund Project of Humanities and Social Sciences Research of the Ministry of Education in 2019 (9YJAT79010). All procedures conform to the principles outlined in the Declaration of Helsinki and Ethics committee of Islamic Azad University of Kerman Branch has approved the experiments.

## References

- 1 J. Wu, X. Wang, M. Khatami, M. S. Nejad, S. Salari and P. G. N. Zhu, *IET Nanobiotechnol.*, 2016, **10**, 237.
- 2 J. M. Granjeiro, R. Cruz, P. E. Leite, S. Gemini-Piperni, L. C. Boldrini and A. R. Ribeiro, *Tin Oxide Materials*, Elsevier, 2020, p. 133.
- 3 J. Han, L. Xiong, X. Jiang, X. Yuan, Y. Zhao and D. Yang, *Prog. Polym. Sci.*, 2019, **91**, 1.
- 4 S. Pramanik and D. Sundar Das, *Two-Dimensional Nanostructures for Biomedical Technology*, Elsevier, 2020, p. 281.
- 5 P. Liu, J. R. Williams and J. J. Cha, *Nat. Rev. Mater.*, 2019, **4**, 479.
- 6 A. Zengin, P. Sutthavas and S. van Rijt, *Nanostructured Biomaterials for Regenerative Medicine*, Woodhead Publishing, 2020, p. 293.
- 7 M. Chen, Y. Sun, J. Liang, G. Zeng, Z. Li, L. Tang and B. Song, *Environ. Int.*, 2019, **126**, 690.
- 8 B. Noorani, F. Tabandeh, F. Yazdian, Z. S. Soheili, M. Shakibaie and S. Rahmani, *Int. J. Polym. Mater. Polym. Biomater.*, 2018, **64**, 754.
- 9 Z. Meng, R. M. Stoltz, L. Mendecki and K. A. Mirica, *Chem. Rev.*, 2019, **119**, 478.
- 10 R. Fang, M. Liu and L. Jiang, *Nano Today*, 2019, **24**, 48.
- 11 G. J. Boelen, L. Boute, J. d'Hoop, M. EzEldeen, I. Lambrichts and G. Opdenakker, *Clin. Oral. Investig.*, 2019, **23**, 2823.
- 12 Y. Zhang and B. R. Lawn, *J. Dent. Res.*, 2018, **97**, 140.
- 13 B. Duane, S. Harford, D. Ramasubbu, R. Stancliffe, E. Pasdeki-Clewer, R. Lomax and I. Steinbach, *Br. Dent. J.*, 2019, **226**, 292.
- 14 F. Mirsiaghi, A. Leung, P. Fine, R. Blizzard and C. Louca, *Br. Dent. J.*, 2018, **225**, 420.
- 15 N. Monteiro, G. Thrivikraman, A. Athirasala, A. Tahayeri, C. M. França, J. L. Ferracane and L. E. Bertassoni, *Dent. Mater.*, 2018, **34**, 389.
- 16 G. J. Boelen, L. Boute, J. d'Hoop, M. EzEldeen, I. Lambrichts and G. Opdenakker, *Clin. Oral. Investig.*, 2019, **23**, 2823.
- 17 A. Schneider, J. Andrade, K. Tanja-Dijkstra and D. R. Moles, *J. Anxiety. Disord.*, 2018, **58**, 33.
- 18 I. Ferreira, C. L. Vidal, A. L. Botelho, P. S. Ferreira, M. L. da Costa Valente, M. A. Schiavon, O. L. Alves and A. Cândido dos Reis, *J. Prosthet. Dent.*, 2020, **123**, 529.
- 19 H. Amini, J. D. Shenkin and D. L. Chi, *Pediatr. Dent.*, 2019, **159**, 617.
- 20 N. Thomas, S. Blake, C. Morris and D. R. Moles, *Int. J. Paediatr. Dent.*, 2018, **28**, 226.
- 21 S. Sudenthiran, V. A. Ganesh, S. Harinee and M. Jacob, *J. Dent. Educ.*, 2018, **3**, 6.
- 22 G. Staunton and J. Hyland, *J. Ir. Dent. Assoc.*, 2018, **64**, 30.
- 23 M. Salas, C. Lucena, L. J. Herrera, A. Yebra, A. Della Bona and M. M. Pérez, *Dent. Mater.*, 2018, **34**, 1168.
- 24 I. Mirghani, F. Mushtaq, M. J. Allsop, L. M. Al-Saud, N. Tickhill, C. Potter and M. Manogue, *Eur. J. Dent. Educ.*, 2018, **22**, 67.



25 M. Eichenberger, N. Biner, M. Amato, A. Lussi and P. Perrin, *Operat. Dent.*, 2018, **43**, 501.

26 L. E. Silva Soares, S. Nahórny, V. de Faria Braga, F. Roberta Marciano, T. T. Bhattacharjee and A. Oliveira Lobo, *Spectrochim. Acta, Part A*, 2020, **228**, 117818.

27 Y. Hassona, D. Malamos, M. Shaqman, Z. Baqain and C. Scully, *Oral Dis.*, 2018, **24**, 228.

28 J. Burns, N. McGoldrick and M. Muir, *Evid. Based Dent.*, 2018, **19**, 69.

29 C. T. Chang, G. R. Badger, B. Acharya, A. F. Gaw, M. S. Barratt and B. T. Chiquet, *Pediatr. Dent.*, 2018, **40**, 265.

30 M. E. Harb, S. Ebrahim, M. Soliman and M. Shabana, *J. Electron. Mater.*, 2018, **47**, 353.

31 S. Palazzolo, S. Bayda, M. Hadla, I. Caligiuri, G. Corona, G. Toffoli and F. Rizzolio, *Curr. Med. Chem.*, 2018, **25**, 4224.

32 Y. Y. Broza, R. Vishinkin, O. Barash, M. K. Nakhleh and H. Haick, *Chem. Soc. Rev.*, 2018, **47**, 4781.

33 Y. Yu, Y. Shi and B. Zhang, *Acc. Chem. Res.*, 2018, **51**, 1711.

34 M. Oveis, M. A. Asli and N. M. Mahmoodi, *J. Hazard. Mater.*, 2018, **347**, 123.

35 R. S. Andre, R. C. Sanfelice, A. Pavinatto, L. H. Mattoso and D. S. Correa, *Mater. Des.*, 2018, **156**, 154.

36 J. Zhu, J. Hou, Y. Zhang, M. Tian, T. He, J. Liu and V. Chen, *J. Membr. Sci.*, 2018, **550**, 173.

37 P. Makvandi, J. T. Gu, E. Nazarzadeh Zare, B. Ashtari, A. Moeini, F. R. Tay and L. N. Niu, *Acta Biomater.*, 2020, **101**, 69.

38 S. Palazzolo, S. Bayda, M. Hadla, I. Caligiuri, G. Corona, G. Toffoli and F. Rizzolio, *Curr. Med. Chem.*, 2018, **25**, 4224.

39 Y. Chen, Z. Fan, Z. Zhang, W. Niu, C. Li, N. Yang and H. Zhang, *Chem. Rev.*, 2018, **118**, 6409.

40 H. Cheng, N. Yang, Q. Lu, Z. Zhang and H. Zhang, *Adv. Mater.*, 2018, **30**, 1707189.

41 K. A. Roach, A. B. Stefaniak and J. R. Roberts, *J. Immunotoxicol.*, 2019, **16**, 87.

42 D. Zhang, C. Zhang, J. Liu, Q. Chen, X. Zhu and C. Liang, *ACS Appl. Nano Mater.*, 2018, **2**, 28.

43 L. Aline Pires, L. J. de Azevedo Silva, B. M. Ferrairo, R. Erbereli, J. F. Parreira Lovo, O. Ponce Gomes, J. Henrique Rubo, P. N. Lisboa-Filho, J. A. Griggs, C. A. Fortulan and A. F. Sanches Borges, *Dent. Mater.*, 2020, **36**, 38.

44 E. J. Foster, N. Zahed and C. Tallon, *Small*, 2018, **14**, 1870215.

45 D. H. Jung, A. Sharma and J. P. Jung, *J. Alloys Compd.*, 2018, **743**, 300.

46 M. Singh, M. Goyal and K. Devlal, *J. Taibah Univ. Sci.*, 2018, **12**, 470.

47 Q. Cai, K. Subramani, R. T. Mathew and X. Yang, *Nanobiomaterials in Clinical Dentistry*, Elsevier, Second edition, 2019, p. 429.

48 A. J. Clancy, M. K. Bayazit, S. A. Hodge, N. T. Skipper, C. A. Howard and M. S. Shaffer, *Chem. Rev.*, 2018, **118**, 7363.

49 K. Ghosal and K. Sarkar, *ACS Biomater. Sci. Eng.*, 2018, **4**, 2653.

50 M. Z. Islam Nizami, S. Takashiba and Y. Nishina, *Appl. Mater. Today*, 2020, **19**, 100576.

51 A. J. Clancy, M. K. Bayazit, S. A. Hodge, N. T. Skipper, C. A. Howard and M. S. Shaffer, *Chem. Rev.*, 2018, **118**, 7363.

52 R. Rao, C. L. Pint, A. E. Islam, R. S. Weatherup, S. Hofmann, E. R. Meshot and J. Carpena-Nuñez, *ACS Nano*, 2018, **12**, 11756.

53 P. Laux, C. Riebeling, A. M. Booth, J. D. Brain, J. Brunner, C. Cerrillo and H. Jungnickel, *Environ. Sci.*, 2018, **5**, 48.

54 B. Yang, M. Zhang, Z. Lu, J. Luo, S. Song and Q. Zhang, *ACS Sustainable Chem. Eng.*, 2018, **6**, 8954.

55 J. Bott and R. Franz, *Appl. Sci.*, 2019, **9**, 214.

56 N. R. Panda, S. P. Pati and D. Das, *Appl. Surf. Sci.*, 2019, **491**, 313.

57 P. Khade, T. Bagwaiya, S. Bhattacharya, A. Singh, P. Jha and V. Shelke, *AIP Conf. Proc.*, 2018, **1942**, 110052.

58 S. A. Bello, J. O. Agunsoye, J. A. Adebisi and S. B. Hassan, *Eng. Appl. Sci. Res.*, 2018, **45**, 262.

59 A. Marcovici, G. Le Saux, V. Bhingardive, P. Rukenstein, K. Flomin, K. Shreth and M. Schwartzman, *ACS Nano*, 2018, **12**, 10016.

60 A. Bera, A. Bhattacharya, N. Tiwari, S. N. Jha and D. Bhattacharyya, *Surf. Sci.*, 2018, **669**, 145.

61 R. J. Varghese, S. Parani, S. Thomas, O. S. Oluwafemi and J. Wu, *Nanomater. Sol. Cell Appl.*, 2019, **2019**, 75–95.

62 S. A. Davari, J. L. Gottfried, C. Liu, E. L. Ribeiro, G. Duscher and D. Mukherjee, *Appl. Surf. Sci.*, 2019, **473**, 156.

63 X. Wang, H. Li, M. Li, C. Li, H. Dai and B. Yang, *Diamond Relat. Mater.*, 2018, **86**, 179.

64 W. Shang, T. Cai, Y. Zhang, D. Liu and S. Liu, *Tribol. Int.*, 2018, **118**, 373.

65 F. Cazaña, N. Latorre, P. Tarifa, J. Labarta, E. Romeo and A. Monzón, *Catal. Today*, 2018, **299**, 67.

66 J. Lin, Y. He, X. Du, Q. Lin, H. Yang and H. Shen, *Crystals*, 2018, **8**, 384.

67 H. Mao and B. Li, *Nano*, 2018, **13**, 1850027.

68 M. Catauro, E. Tranquillo, G. Dal Poggetto, M. Pasquali, A. Dell'Era and S. Vecchio Cipriotti, *Materials*, 2018, **11**, 2364.

69 F. Ansari, A. Sobhani and M. J. Salavati-Niasari, *Colloid Interface Sci.*, 2018, **514**, 723.

70 T. Budnyak, S. Aminzadeh, I. Pylypchuk, A. Riazanova, V. Tertykh, M. Lindström and O. Sevastyanova, *Nanomater.*, 2018, **8**, 950.

71 C. Aydin, *J. Mater. Sci.*, 2018, **29**, 20087.

72 G. Molnár, S. Rat, L. Salmon, W. Nicolazzi and A. Bousseksou, *Adv. Mater.*, 2018, **30**, 1703862.

73 J. M. Salva, D. D. Gutierrez, L. A. Ching, P. M. Ucab, H. Cascon and N. P. Tan, *Nanotechnol.*, 2018, **29**, 50LT01.

74 B. Náfrádi, M. Choucair and L. Forró, *Nanomater.*, 2018, **1**, 67.

75 W. Tian, S. Liu, L. Deng, N. Mahmood and X. Jian, *Composites*, 2018, **149**, 92–98.

76 N. A. Tien, C. H. Diem, N. T. T. Linh, V. O. Mittova and I. Y. Mittova, *Nanosystems*, 2018, **9**, 424.

77 Y. Manawi, A. Samara, T. Al-Ansari and M. Atieh, *Materials*, 2018, **11**, 822.

78 R. Atchudan, T. N. J. I. Edison, S. Perumal, D. RanjithKumar and Y. R. Lee, *Int. J. Hydrogen Energy*, 2019, **44**, 2349.



79 W. Shang, T. Cai, Y. Zhang, D. Liu and S. Liu, *Tribol. Int.*, 2018, **118**, 373.

80 S. Nizamuddin, M. T. H. Siddiqui, N. M. Mubarak, H. A. Baloch, S. A. Mazari, M. M. Tunio and S. Riaz, *Curr. Org. Chem.*, 2018, **22**, 446.

81 S. Kalaiselvan, K. Balachandran, S. Karthikeyan and R. Venkatesh, *Silicon*, 2018, **10**, 211.

82 Z. Guo, K. Cui, G. Zeng, J. Wang and X. Guo, *Sci. Environ.*, 2018, **643**, 1325.

83 Y. Chen, Z. Fan, Z. Zhang, W. Niu, C. Li, N. Yang and H. Zhang, *Chem. Rev.*, 2018, **118**, 6409.

84 J. Yao, H. Wang, M. Chen and M. Yang, *Microchim. Acta*, 2019, **186**, 395.

85 M. S. Zafar, A. A. Alnazzawi, M. Alrahabi, M. A. Fareed, S. Najeeb and Z. Khurshid, *Adv. Dent. Biomater.*, 2019, **18**, 477.

86 X. Gao and G. V. Lowry, *NanoImpact*, 2018, **9**, 14.

87 J. Wang, R. Chen, L. Xiang and S. Komarneni, *Ceram. Int.*, 2018, **44**, 7357.

88 M. L. Cui, Y. S. Chen, Q. F. Xie, D. P. Yang and M. Y. Han, *Coord. Chem. Rev.*, 2019, **387**, 450.

89 Y. Li, Y. Xu, C. C. Fleischer, J. Huang, R. Lin, L. Yang and H. Mao, *J. Mater. Chem.*, 2018, **6**, 9.

90 M. G. Manera, A. Colombelli, A. Taurino, A. G. Martin and R. Rella, *Sci. Rep.*, 2018, **8**, 12640.

91 A. Besinis, T. De Peralta, C. J. Tredwin and R. D. Handy, *ACS Nano*, 2015, **9**, 2255.

92 R. Pokrowiecki, K. Palka and A. Mielczarek, *Nanomedicine*, 2018, **13**, 639.

93 Z. Khurshid, M. Zafar, S. Qasim, S. Shahab, M. Naseem and A. AbuReqaiba, *Materials*, 2015, **8**, 717.

94 H. Fukuda, *Dental implant, US Pat.*, US5174755A, 1992.

95 X. Feng, A. Chen, Y. Zhang, J. Wang, L. Shao and L. Wei, *Int. J. Nanomed.*, 2015, **10**, 3547.

96 D. Elkassas and A. Arafa, *Nanomed.*, 2017, **13**, 1543.

97 M. Hannig and C. Hannig, *Nanobiomater. Clin. Dent.*, 2019, **201**, 1.

98 M. Goldberg, *Dentistry and Oral Health Care*, 2018, **1**, 19.

99 D. R. Schwass, K. M. Lyons, R. Love, G. R. Tompkins and C. J. Meledandri, *Adv. Dent. Res.*, 2018, **29**, 117.

100 C. O. Favretto, A. C. B. Delbem, J. C. S. Moraes, E. R. Camargo, P. T. A. de Toledo and D. Pedrini, *Clin. Oral Investig.*, 2018, **1**, 3021–3029.

101 V. Manikandan, P. Velmurugan, J. H. Park, W. S. Chang, Y. J. Park, P. Jayanthi and B. T. Oh, *Biotech*, 2017, **7**, 72.

102 A. Mackevica, M. E. Olsson and S. F. Hansen, *J. Hazard. Mater.*, 2017, **322**, 270.

103 M. Ibrahim, F. AlQarni, Y. Al-Dulaijan, M. Weir, T. Oates, H. Xu and M. Melo, *Materials*, 2018, **11**, 1544.

104 M. O. Wassel and M. A. Khattab, *J. Adv. Res.*, 2017, **8**, 387.

105 S. Nguyen, C. Escudero, N. Sediqi, G. Smistad and M. Hiorth, *Eur. J. Pharm. Sci.*, 2017, **104**, 326.

106 J. B. Fathima, A. Pugazhendhi and R. Venis, *Microb. Pathog.*, 2017, **110**, 245.

107 H. Wang, Z. Xiao, J. Yang, D. Lu, A. Kishen, Y. Li and X. Yang, *Sci. Rep.*, 2017, **7**, 40701.

108 Y. Liu, P. C. Naha, G. Hwang, D. Kim, Y. Huang, A. Simon-Soro and F. Alawi, *Nat. Commun.*, 2018, **9**, 2920.

109 S. Jahanizadeh, F. Yazdian, A. Marjani, M. Omidi and H. Rashedi, *Int. J. Biol. Macromol.*, 2017, **105**, 757.

110 Y. A. Al-Dulaijan, L. Cheng, M. D. Weir, M. A. S. Melo, H. Liu, T. W. Oates and H. H. Xu, *J. Dent.*, 2018, **72**, 44.

111 H. Yan, H. Yang, K. Li, J. Yu and C. Huang, *Molecules*, 2017, **22**, 1225.

112 A. Maghsoudi, F. Yazdian, S. Shahmoradi, L. Ghaderi, M. Hemati and G. Amoabediny, *Mater. Sci. Eng.*, 2017, **75**, 1259.

113 C. Covarrubias, D. Trepiana and C. Corral, *Dent. Mater. J.*, 2018, **37**, 379.

114 A. Gitipour, S. R. Al-Abed, S. W. Thiel, K. G. Scheckel and T. Tolaymat, *Chemosphere*, 2017, **173**, 245.

115 A. C. Ionescu, S. Hahnel, G. Cazzaniga, M. Ottobelli, R. R. Braga, M. C. Rodrigues and E. Brambilla, *J. Mater. Sci.*, 2017, **28**, 108.

116 M. Joana, M. Francisco, F. Ana, B. Maria João, M. Paulo Durão and R. José Alexandre, *Ann. Med.*, 2019, **51**, 130.

117 R. B. Anchieta, I. A. E. Hoshino, A. C. F. Júnior, E. O. de Almeida, E. P. Rocha and W. G. Assunção, *J. Dent. Implants*, 2019, **9**, 41.

118 H. J. A. Judy, *Dent. J.*, 2018, **6**, 172.

119 E. E. Totu, A. C. Nechifor, G. Nechifor, H. Y. Aboul-Enein and C. M. Cristache, *J. Dent.*, 2017, **59**, 68.

120 A. P. R. Magalhães, C. A. Fortulan, P. N. Lisboa-Filho, C. M. Ramos-Tonello, O. P. Gomes, P. F. Cesar and A. F. S. Borges, *Ceram. Int.*, 2018, **44**, 2959.

121 M. M. Gad, R. Abualsaud, A. Rahoma, A. M. Al-Thobity, K. S. Al-Abidi and S. Akhtar, *Int. J. Nanomed.*, 2018, **13**, 283.

122 M. Sarraf, A. Dabbagh, B. A. Razak, R. Mahmoodian, B. Nasiri-Tabrizi, H. R. Hosseini and N. L. Sukiman, *Surf. Coat. Technol.*, 2018, **349**, 1008.

123 U. F. Gunputh, H. Le, R. D. Handy and C. Tredwin, *Mater. Sci. Eng.*, 2018, **91**, 638.

124 Y. Yang, S. Ren, X. Zhang, Y. Yu, C. Liu, J. Yang and L. Miao, *Int. J. Nanomed.*, 2018, **13**, 3751.

125 J. M. Jang, S. D. Kim, T. E. Park and H. C. Choe, *Appl. Surf. Sci.*, 2018, **432**, 285.

126 J. Rosenbaum, D. L. Versace, S. Abbad-Andallousi, R. Pires, C. Azevedo, P. Cénédese and P. Dubot, *Biomater. Sci.*, 2017, **5**, 455.

127 Z. G. Azzawi, T. I. Hamad, S. A. Kadhim and G. A. H. Naji, *J. Mater. Sci.*, 2018, **29**, 96.

128 S. Kim, C. Park, K. H. Cheon, H. D. Jung, J. Song, H. E. Kim and T. S. Jang, *Appl. Surf. Sci.*, 2018, **451**, 232.

129 M. Boutinguiza, M. Fernández-Arias, J. del Val, J. Buxaderas-Palomero, D. Rodríguez, F. Lusquiños and J. Pou, *Mater. Lett.*, 2018, **231**, 126.

130 D. D. Divakar, N. T. Jastaniyah, H. G. Altamimi, Y. O. Alnakhli, A. A. Alkheraif and S. Haleem, *Int. J. Biol. Macromol.*, 2018, **108**, 790.

131 Y. Xiang, J. Li, X. Liu, Z. Cui, X. Yang, K. W. K. Yeung and S. Wu, *Mater. Sci. Eng.*, 2017, **79**, 629.



132 K. Jadhav, H. R. Rajeshwari, S. Deshpande, S. Jagwani, D. Dhamecha, S. Jalalpure and D. Baheti, *Mater. Sci. Eng.*, 2018, **93**, 664.

133 J. J. Segura-Egea, K. Gould, B. H. Şen, P. Jonasson, E. Cotti, A. Mazzoni and P. M. H. Dummer, *Int. Endod. J.*, 2018, **51**, 20.

134 N. H. F. Wilson, F. J. T. Burke, P. A. Brunton, S. Creanor, M. T. Hosey and F. Mannocci, *Br. Dent. J.*, 2019, **226**, 110.

135 K. Pineda, R. Bueno, C. Alvarado, F. Abella, M. Roig and F. Duran-Sindreu, *Aust. Endod. J.*, 2018, **44**, 40.

136 A. Torres, E. Shaheen, P. Lambrechts, C. Politis and R. Jacobs, *Int. Endod. J.*, 2019, **52**, 540.

137 S. G. Kim, M. Malek, A. Sigurdsson, L. M. Lin and B. Kahler, *Int. Endod. J.*, 2018, **51**, 1367.

138 S. Xiao, K. Liang, M. Weir, L. Cheng, H. Liu, X. Zhou and H. Xu, *Materials*, 2017, **10**, 89.

139 C. T. Rodrigues, F. B. de Andrade, L. R. S. M. de Vasconcelos, R. Z. Midena, T. C. Pereira, M. C. Kuga and N. Bernardineli, *Int. Endod. J.*, 2018, **51**, 901.

140 S. Bulkhari, D. Kim, Y. Liu, B. Karabucak and H. Koo, *J. Endod.*, 2018, **44**, 806.

141 N. J. M. Opdam, K. Collares, R. Hickel, S. C. Bayne, B. A. Loomans, M. S. Cenci and N. H. F. Wilson, *Dent. Mater.*, 2018, **34**, 1.

142 W. F. Waggoner and T. Nelson, *Pediatr. Dent.*, 2019, 304.

143 F. Schwendicke and N. Opdam, *Dent. Mater.*, 2018, **34**, 29.

144 R. Sarkis-Onofre, T. Pereira-Cenci, A. C. Tricco, F. F. Demarco, D. Moher and M. S. Cenci, *Journal of Esthetic and Restorative Dentistry*, 2019, **31**, 222.

145 G. P. Ramiro, C. A. Coronel, A. F. Navarro, B. Hassan and F. Tamimi, *Digit. Restor. Dent.*, 2019, **41**, 7–39.

146 J. A. Rodrigues, L. Casagrande, F. B. Araújo, T. L. Lenzi and A. A. Mariath, *Pediatr. Restor. Dent.*, 2019, 161.

147 T. E. Donovan, R. Marzola, K. R. Murphy, D. R. Cagna, F. Eichmiller, J. R. McKee and M. Troeltzsche, *J. Prosthet. Dent.*, 2018, **120**, 816.

148 A. Abdullah, F. Muhammed, B. Zheng and Y. Liu, *J. Dent. Mater. Tech.*, 2018, **7**, 1.

149 S. J. Lee, M. Heo, D. Lee, S. Han, J. H. Moon, H. N. Lim and I. K. Kwon, *Appl. Surf. Sci.*, 2018, **432**, 317.

150 W. Cao, X. Wang, Q. Li, Z. Ye and X. Xing, *Mater. Lett.*, 2018, **220**, 104.

151 W. Cao, Y. Zhang, X. Wang, Y. Chen, Q. Li, X. Xing and Z. Ye, *J. Mater. Sci.*, 2017, **28**, 103.

152 Y. Zhang, C. Huang and J. Chang, *J. Mater. Chem.*, 2018, **6**, 477.

153 P. Cevik and A. Z. Yildirim-Bicer, *J. Prosthodontics*, 2018, **27**, 763.

154 L. Ghahremani, S. Shirkavand, F. Akbari and N. Sabzikari, *J. Clin. Experiment. Dent.*, 2017, **9**, e661.

155 A. Sodagar, M. S. A. Akhoundi, A. Bahador, Y. F. Jalali, Z. Behzadi, F. Elhaminejad and A. H. Mirhashemi, *Dental Press J. Orthodont.*, 2017, **22**, 67.

156 M. C. Rodrigues, M. D. Chiari, Y. Alania, L. C. Natale, V. E. Arana-Chavez, M. M. Meier and R. R. Braga, *Dent. Mater.*, 2018, **34**, 746.

157 A. Meena, H. S. Mali, A. Patnaik and S. R. Kumar, *Polym. Chem.*, 2018, **39**, E321.

158 M. S. Al-Ajely, K. M. Ziadan and R. M. Al-Bader, *Int. J. Res. Granthaalayah*, 2018, **6**, 338.

159 L. M. Campos, L. C. Boaro, T. M. Santos, V. J. Santos, R. Grecco-Romano, M. J. Santos and D. F. Parra, *J. Therm. Anal. Calorim.*, 2018, **131**, 771.

160 R. M. Al-Mosawi and R. M. Al-Badr, *IOSR J. Dent. Med. Sci.*, 2017, **16**, 49.

161 D. L. Yang, J. Xiao, D. Wang, W. M. Lin, Y. Pu, X. F. Zeng and J. X. Wang, *Ind. Eng. Chem. Res.*, 2018, **57**, 12809.

162 H. B. Dias, M. I. B. Bernardi, T. M. Bauab, A. C. Hernandes and A. N. de Souza Rastelli, *Dent. Mater.*, 2019, **35**, e36.

163 M. Ai, Z. Du, S. Zhu, H. Geng, X. Zhang, Q. Cai and X. Yang, *Dent. Mater.*, 2017, **33**, 12.

164 Y. Wang, H. Hua, W. Li, R. Wang, X. Jiang and M. Zhu, *J. Dent.*, 2019, **80**, 23.

165 R. Wang, E. Habib and X. X. Zhu, *Dent. Mater.*, 2017, **33**, 1139.

166 L. Paiva, T. K. S. Fidalgo, L. P. da Costa, L. C. Maia, L. Balan, K. Anselme and R. M. S. M. Thiré, *J. Dent.*, 2018, **69**, 102.

167 D. Sundeep, T. V. Kumar, P. S. Rao, R. V. S. S. N. Ravikumar and A. G. Krishna, *Prog. Biomater.*, 2017, **6**, 57.

168 P. P. N. S. Garcia, M. F. B. Cardia, R. S. Francisconi, L. N. Dovigo, D. M. P. Spolidório, A. N. de Souza Rastelli and A. C. Botta, *Microsc. Res. Tech.*, 2017, **80**, 456.

169 C. A. Stewart, J. H. Hong, B. D. Hatton and Y. Finer, *Acta Biomater.*, 2018, **76**, 283.

170 B. Han, W. Xia, K. Liu, F. Tian, Y. Chen, X. Wang and Z. Yang, *ACS Appl. Mater. Interfaces*, 2018, **10**, 8519.

171 E. Azad, M. Atai, M. Zandi, P. Shokrollahi and L. Solhi, *Dent. Mater.*, 2018, **34**, 1263.

172 Y. Liu, L. Zhang, L. N. Niu, T. Yu, H. H. Xu, M. D. Weir and J. H. Chen, *J. Dent.*, 2018, **72**, 53.

173 S. Yue, J. Wu, Q. Zhang, K. Zhang, M. D. Weir, S. Imazato and H. H. Xu, *J. Dent.*, 2018, **75**, 48.

174 F. D. Al-Qarni, F. Tay, M. D. Weir, M. A. Melo, J. Sun, T. W. Oates and H. H. Xu, *J. Dent.*, 2018, **78**, 91.

175 X. Xie, L. Wang, D. Xing, K. Zhang, M. D. Weir, H. Liu and H. H. Xu, *Dent. Mater.*, 2017, **33**, 553.

176 K. Liang, S. Xiao, M. D. Weir, C. Bao, H. Liu, L. Cheng and H. H. Xu, *J. Biomed. Mater. Res.*, 2018, **106**, 2414.

177 M. Dutra-Correia, A. A. Leite, S. P. de Cara, I. M. Diniz, M. M. Marques, I. B. Suffredini and I. S. Medeiros, *J. Dent.*, 2018, **77**, 66.

178 R. Thomas, S. Snigdha, K. B. Bhavitha, S. Babu, A. Ajith and E. K. Radhakrishnan, *Biotech.*, 2018, **8**, 404.

179 J. Sun and W. L. Wu, inventor, Google Patents, assignee. Toothpaste patent US20120172485A1, 2012.

180 B. M. Priyadarshini, K. Mitali, T. B. Lu, H. K. Handral, N. Dubey and A. S. Fawzy, *Dent. Mater.*, 2017, **33**, 830.

181 M. F. Gutiérrez, P. Malaquias, T. P. Matos, A. Szesz, S. Souza and J. Bermudez, *Dent. Mater.*, 2018, **33**, 309.

182 M. F. Gutiérrez, P. Malaquias, V. Hass, T. P. Matos, L. Lourenço and A. Reis, *J. Dent.*, 2019, **61**, 12–20.



183 G. A. Frolov, Y. N. Karasenkov, A. A. Gusev, O. V. Zakharova, A. Y. Godymchuk, D. V. Kuznetsov and V. K. Leont'ev, *Nano Hybrids and Composites*, 2017, **13**, 39–46.

184 M. Rizk, L. Hohlfeld, L. T. Thanh, R. Biehl, N. Lühmann, D. Mohn and A. Wiegand, *Dent. Mater.*, 2017, **33**, 1056–1065.

185 V. Velkoborsky, inventor, Google Patents, assignee. Toothpaste patent US20100239618 A1, 2010.

186 S. Prakasam, P. Gajendrareddy, C. Louie, C. Lee and L. E. Bertassoni, *Biomater. Immune Response*, 2018, 211.

187 E. T. Knight and W. Murray Thomson, *Periodontol*, 2018, **78**, 195.

188 J. G. Deeb, C. K. Carrico, D. M. Laskin and T. E. Koertge, *J. Dent. Educ.*, 2019, **83**, 457.

189 G. Zucchelli, P. Sharma and I. Mounssif, *Periodontol*, 2018, **77**, 7–18.

190 Z. Danish, M. N. Shah, S. Rehmat, F. A. Hakam and H. A. Raza, *Dent. J.*, 2019, **39**, 60.

191 S. N. Papageorgiou, G. N. Antonoglou, C. Martin and T. Eliades, *J. Orthod.*, 2019, **46**, 101.

192 A. S. Khan, A. N. Hussain, L. Sidra, Z. Sarfraz, H. Khalid, M. Khan and I. U. Rehman, *Mater. Sci. Eng.*, 2017, **80**, 387.

193 D. K. Khajuria, S. F. Zahra and R. Razzan, *J. Biomater. Sci.*, 2018, **29**, 74.

194 C. Mahapatra, R. K. Singh, J. H. Lee, J. Jung, J. K. Hyun and H. W. Kim, *Acta Biomater.*, 2017, **50**, 142.

195 Y. Xia, H. Chen, F. Zhang, L. Wang, B. Chen, M. A. Reynolds and H. H. Xu, *Artif. Cells, Nanomed., Biotechnol.*, 2018, **46**, 423.

196 Y. Ji, S. K. Choi, A. S. Sultan, K. Chuncai, X. Lin, E. Dashtimoghadam and Z. Nie, *Nanomed*, 2018, **14**, 919.

197 Y. Xia, H. Chen, F. Zhang, C. Bao, M. D. Weir, M. A. Reynolds and H. H. Xu, *Nanomed*, 2018, **14**, 35.

198 A. L. Popov, O. G. Tatarnikova, N. R. Popova, I. I. Selezneva, A. Y. Akkizov, A. M. Ermakov and V. K. Ivanov, *Nano Hybrids and Composites*, 2017, **13**, 26.

199 C. Y. Huang, T. H. Huang, C. T. Kao, Y. H. Wu, W. C. Chen and M. Y. Shie, *J. Endod.*, 2017, **43**, 69.

200 M. Ates, Z. Arslan, V. Demir, J. Daniels and I. O. Farah, *Environ. Toxicol.*, 2015, **30**, 119.

201 M. Coccia and L. Wang, *Proc. Natl. Acad. Sci. U. S. A.*, 2016, **113**, 2057.

202 M. Giovanni, C. Y. Tay, M. I. Setyawati, J. Xie, C. N. Ong, R. Fan and D. T. Leong, *Environ. Toxicol.*, 2015, **30**, 1459.

203 M. Coccia, *Scientometrics*, 2018, **117**, 1265.

204 L. Li, T. Liu, C. Fu, L. Tan, X. Meng and H. Liu, *Nanomed*, 2015, **11**, 1915.

205 M. Coccia, *Tech. Soc.*, 2020, **60**, 1.

206 I. Y. Kim, E. Joachim, H. Choi and K. Kim, *Nanomed*, 2015, **11**, 407.

207 N. Klinthoophamrong, D. Chaikiawkeaw, W. Phoolcharoen, K. Rattanapisit, P. Kaewpungsup, P. Pavasant and V. P. Hoven, *Int. J. Biol. Macromol.*, 2020, **149**, 51.

208 M. Coccia, *Int. J. Healthc. Tech. Manag.*, 2012, **13**, 184.

209 X. Jing, J. H. Park, T. M. Peters and P. S. Thorne, *Toxicol.*, 2015, **29**, 502.

210 M. Coccia, U. Finardi and D. Margon, *J. Technol. Trans.*, 2012, **37**, 777.

211 N. Adam, A. Vakurov, D. Knapen and R. Blust, *J. Hazard. Mater.*, 2015, **283**, 416.

212 G. Libralato, G. Lofrano, A. Siciliano, E. Gambino, G. Boccia, C. Federica, A. Francesco, E. Galdiero, R. Gesuele and M. Guida, *Visible Light Active Structured Photocatalysts for the Removal of Emerging Contaminants*, Elsevier, 2020, p. 195.

213 M. Coccia and J. Watts, *J. Eng. Tech. Manag.*, 2020, **55**, 101552.

214 M. Kumari, S. P. Singh, S. Chinde, M. F. Rahman, M. Mahboob and P. Grover, *Int. J. Toxicol.*, 2014, **33**, 86.

215 M. Coccia, *Technol. Forecast. Soc. Change*, 2019, **141**, 289.

216 S. Aalapati, S. Ganapathy, S. Manapuram, G. Anumolu and B. M. Prakya, *Nanotoxicol*, 2014, **8**, 786.

217 M. Coccia, *Technol. Anal. Strateg. Manage.*, 2017, **29**, 1048.

218 B. Collin, E. Oostveen, O. V. Tsyusko and J. M. Unrine, *Environ. Sci. Technol.*, 2014, **48**, 1280.

219 E. O. Ogunsona, R. Muthuraj, E. Ojogbo, O. Valerio and T. H. Mekonnen, *Appl. Mater. Today*, 2020, **18**, 100473.

220 M. Coccia, *Technol. Anal. Strateg. Manage.*, 2014, **26**, 733.

221 N. S. Taylor, R. Merrifield, T. D. Williams, J. K. Chipman, J. R. Lead and M. R. Viant, *Nanotoxicol*, 2016, **10**, 32.

222 R. Abbasalipourkabir, H. Moradi, S. Zarei, S. Asadi, A. Salehzadeh, A. Ghafourikhosroshahi and N. Ziamajidi, *Food Chem. Toxicol.*, 2015, **84**, 154.

223 N. R. Jacobsen, T. Stoeger, S. Van Den Brûle, A. T. Saber, A. Beyerle, G. Vietti and A. Banerjee, *Food Chem. Toxicol.*, 2015, **85**, 84.

224 T. Y. Suman, S. R. Rajasree and R. Kirubagaran, *Ecotoxicol. Environ.*, 2015, **113**, 23.

225 J. Choi, H. Kim, P. Kim, E. Jo, H. M. Kim, M. Y. Lee and K. Park, *J. Toxicol. Environ. Health*, 2015, **78**, 226.

226 Q. Fang, X. Shi, L. Zhang, Q. Wang, X. Wang, Y. Guo and B. Zhou, *J. Hazard. Mater.*, 2015, **283**, 897.

227 N. R. B. Younes, S. Amara, I. Mrad, I. Ben-Slama, M. Jeljeli, K. Omri and M. Sakly, *Environ. Sci. Pollut. Res.*, 2015, **22**, 8728.

228 Z. L. Wang, *MRS Bull.*, 2007, **32**, 109.

229 A. Ghasempour Ardakani and P. Rafieipour, *J. Opt. Soc. Am. B*, 2018, **35**, 1708.

230 D. B. Rihtnesberg, S. Almqvist, Q. Wang, A. Sugunan, X. Yang, M. S. Toprak, Z. Besharat and M. Göthelid, in *Nanoelectronics Conference*, INEC, 2011, vol. 2011, p. 1.

231 A. Umar, M. M. Rahman, S. H. Kim and Y. B. Hahn, *J. Nanosci. Nanotechnol.*, 2008, **8**, 3216.

232 S. Parasharam, *Mater. Today*, 2013, **16**, 505–506.

